JCI insight

NKX2-5 regulates vessel remodelling in scleroderma-associated pulmonary arterial hypertension

Ioannis Papaioannou, … , David J. Abraham, Markella Ponticos

JCI Insight. 2024. https://doi.org/10.1172/jci.insight.164191.

Research In-Press Preview Pulmonology Vascular biology

Graphical abstract

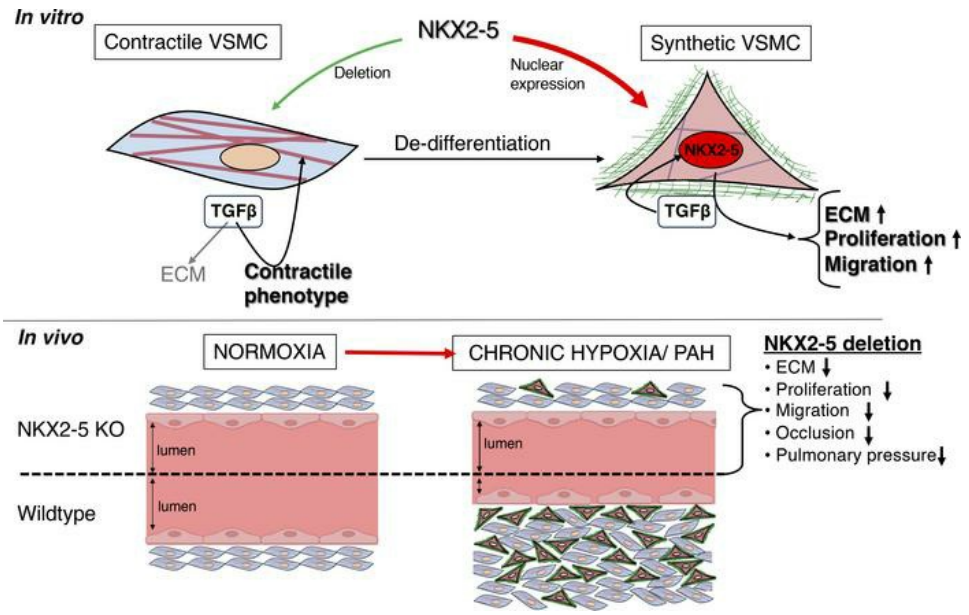

Find the latest version:

https://jci.me/164191/pdf

NKX2-5 regulates vessel remodelling in scleroderma-associated pulmonary arterial hypertension

Ioannis Papaioannou[1], Athina Dritsoula[1], Ping Kang [1], Reshma Baliga[2], Sarah Trinder[1], Emma Cook[1], Xu Shiwen[1], Adrian Hobbs[2], Christopher P. Denton[1], David J. Abraham[1], Markella Ponticos[1],

[1] Division of Medicine, Department of Inflammation, University College London, Royal Free Campus, Rowland Hill Street, London NW3 2PF, UK

[2] William Harvey Research Institute, Barts and The London School of Medicine & Dentistry, Queen Mary University of London, Charterhouse Square, London EC1M 6BQ , UK

Corresponding Author:

Markella Ponticos, Division of Medicine, Department of Inflammation, University College London, Royal Free Campus, Rowland Hill Street, London NW3 2PF, UK

m.ponticos@ucl.ac.uk

Disclosures: The authors have declared that no conflict of interest exists.

Abstract

NKX2-5 is a member of the homeobox-containing transcription factors critical in regulating tissue differentiation in development. Here, we report a role for NKX2-5 in vascular smooth muscle cell phenotypic modulation *in vitro* and in vascular remodelling *in vivo*. NKX2-5 is up-regulated in scleroderma (SSc) patients with pulmonary arterial hypertension. Suppression of NKX2-5 expression in smooth muscle cells, halted vascular smooth muscle proliferation and migration, enhanced contractility and blocked the expression of the extracellular matrix genes. Conversely, overexpression of NKX2-5 suppressed the expression of contractile genes (ACTA2, TAGLN, CNN1) and enhanced the expression of matrix genes (COL1) in vascular smooth muscle cells. *In vivo*, conditional deletion of NKX2-5 attenuated blood vessel remodelling and halted the progression to hypertension in the mouse chronic hypoxia mouse model. This study revealed that signals related to injury such as serum and low confluence, which induce NKX2-5 expression in cultured cells, is potentiated by TGFβ and further enhanced by hypoxia. The effect of TGFβ was sensitive to ERK5 and PI3K inhibition. Our data suggest a pivotal role for NKX2-5 in the phenotypic modulation of smooth muscle cells during pathological vascular remodelling and provide proof of concept for therapeutic targeting of NKX2-5 in vasculopathies.

Introduction

Vascular remodelling can be defined as the adaptive structural re-arrangement of blood vessels through alterations in cell growth, survival, and migration, and modulation of the extracellular matrix (ECM) (1-4). Vascular remodelling is involved in embryonic angiogenesis and arteriogenesis. In mature vessels however, it is a consequence of vascular injury and diseases such as atherosclerosis and pulmonary arterial hypertension (PAH). In adult healthy

blood vessels, vascular smooth muscle cells (VSMC) have a low rate of proliferation and ECM synthesis, are largely non-migratory, and are committed to carrying out a contractile function. However, upon vascular injury, 'contractile' VSMC temporarily undergo phenotypic modulation to a highly proliferative 'synthetic' phenotype, which is vital in replacing lost VSMC during vascular repair. The same phenotypic modulation, however, can also contribute to vascular pathology (5), by altering vascular structure in a way that impedes function. This pathologic vascular remodelling is a critical component of most vascular diseases. Heretofore, we shall refer to this proliferative, biosynthetic phenotype as the 'synthetic' phenotype.

Vascular remodelling is of importance in Pulmonary Arterial Hypertension (PAH). PAH, defined as a resting pulmonary artery blood pressure ≥25mmHg, results in dramatic arterial structure alterations, most notably endothelial dysfunction and the over-proliferation of the smooth muscle layer, leading to vessel remodelling and narrowing of the vessel lumen (6-8). As this remodeling process continues, it causes a progressive increase in pulmonary vascular resistance, right ventricular hypertrophy and ultimately right heart failure. The marked remodeling of the pulmonary arteries is believed to result from matrix deposition and proliferation of existing smooth muscle cells. Matrix deposition and proliferation are the hallmarks of the synthetic VSMC phenotype. Chronic hypoxia-induced PAH has been modelled using mice and reproducibly demonstrates many of the features that occur in human PAH.

The molecular mechanism regulating VSMC phenotypic modulation, is incompletely understood. Reports have implicated a number of key transcription factors such as SRF (switching from contractile to the synthetic phenotype and myocardin (migration and proliferation), KLF4 (de-differentiation to the synthetic phenotype), ZEB1 (collagen synthesis repressor maintaining the contractile phenotype) (9-12), yet many questions remain. *In vitro*, phenotypic switch of cultured VSMC to the contractile phenotype can be effectively induced

by serum deprivation or high confluence, which over a period of several days results in strongly increased expression of contractile machinery components and a concomitant reduction in ECM synthesis (5,13).

More recently, seminal work by Chen et al (13), uncovered a role for FGF2 and TGFβ in the maintenance of the contractile phenotype. It appears that TGFβ signalling is essential for the expression of contractile markers and FGF2 exerts direct control over the pathway. Blocking TGFβ prevents cells cultured in serum from reactivating their contractile markers upon serum removal.

NKX2-5 belongs to the highly conserved NK-2 family of homeobox DNA-binding transcription factors (14). Expression of NKX2-5 is one of the earliest markers of the cardiac lineage and is first observed in the developing embryonic heart (15). Targeted disruption of NKX2-5 in mice is lethal, causing the arrest of heart development after the initial stage of cardiac looping (16). A critical role for NKX2-5 in blood vessel development has also been discovered: NKX2-5 is essential for the formation of the major pharyngeal vessels (17). After development, NKX2-5 expression is heart-limited, with undetectable expression in most other tissues such as the lung.

The COL1A2 gene is the rate limiting component for the synthesis of collagen 1 (COL1). Its expression is regulated by two key elements the promoter and an enhancer (18), which respectively control low level expression for maintenance and high-level expression required for extracellular matrix repair or remodelling. Many different cell types, particularly proliferating cells produce COL1 for maintenance and hence the promoter is active in a large variety of tissues. The enhancer on the other hand is only activated in a handful of

mesenchymal cells, such as activated fibroblasts that need to produce large amounts of extracellular matrix (18).

Previously, we discovered, that NKX2-5 expression can be detected in adult collagen-producing VSMC *in vitro* and that it is, in fact, required for activating the COL1A2 enhancer and driving high level collagen expression in VSMC (18). Given that VSMC only express high levels of COL1A2 when they swap to a synthetic phenotype, we investigated the relevance of NKX2-5 re-activation in adult VSMC with respect to VSMC phenotypic modulation. We report that NKX2-5 can indeed be readily detected specifically in synthetic VSMC and not contractile VSMC, coinciding with high levels of COL1A2 expression. We also report that NKX2-5 can be detected in adult remodelled blood vessels from PAH patients, but not in healthy blood vessels, while conditional NKX2-5 deletion inhibits adaptive vascular remodelling in a mouse model of pulmonary hypertension. We propose that PI3K/AKT and ERK5 signalling in response to injury or disease, potentiated by TGFβ signalling, re-activate NKX2-5 in adult blood vessels, enabling some of the cells within the intima to switch to the synthetic phenotype. Although by necessity most of the cells need to remain contractile to maintain vascular tone, having some of the VSMC become synthetic facilitates proliferation and repair. Yet, in doing so, NKX2-5 also licences the overgrowth of the smooth muscle layer, allowing chronic damage signals to induce vascular remodelling. This proposal is supported by our recent finding that NKX2-5 promoter polymorphisms are genetically associated with pulmonary hypertension in scleroderma patients (19).

Results

NKX2-5 expression in human vascular remodelling

We have identified NKX2-5 as an important regulator of collagen 1α2 expression in VSMC (18) through direct activation of the collagen type Iα2 far upstream enhancer, a crucial regulatory element of collagen type I known to be associated with fibrotic disease (20-22). Post-mortem tissue from patients with PAH, was used to test the hypothesis that NKX2-5 is expressed in diseased vessels or vessels undergoing vascular remodelling (**Fig 1**). Using validated specific antibodies (**Supplementary Fig 1**), we observed NKX2-5 expression in the pulmonary vasculature of patients with hypertension (**Fig 1**) as well as in diseased carotid, coronary and peripheral arteries (**Supplementary Fig 2**), where it coincides with ACTA2 expression in VSMC (**Supplementary Fig 2F & G**). In patients with PAH, NKX2-5 is expressed in the media and neointima of large pulmonary arteries (**Fig 1A, left panel**), medium-sized muscularised arterioles (**Fig 1A, upper panel**), and small muscularised arterioles (**Fig 1A, lower panel**). No expression is observed in normal vessels (**Fig 1B &C**). Quantification of NKX2-5 expression revealed that over 70% of cells expressed NKX2-5 in PAH patient pulmonary arteries/arterioles (20-100μm in diameter) compared to under 10% or cells in vessels from control lungs (**Fig 1D**).

NKX2-5 mediates phenotypic modulation of vascular smooth muscle cells

Transition of the normal contractile VSMC in the arterial media towards the synthetic phenotype, is associated with gradual up-regulation of several ECM genes such as collagen type I (COL1), connective tissue growth factor (CCN2) and fibronectin (FN1). Concomitantly, the expression of proteins that are components of the contractile machinery such as ACTA2, TAGLN, CNN1, smooth muscle myosin heavy chain (MYH11) and smoothelin (SMTN) are gradually downregulated.

We cultured human VSMC *in vitro* under conditions favouring either the contractile or synthetic phenotype. Data are shown only for human pulmonary arterial smooth muscle cells (HPASMC) (**Fig 2**), but human aortic smooth muscle cells behaved in a very similar manner (Data not shown). Western blot analyses of total and nuclear lysates revealed that contractile protein (ACTA2, TAGLN, CNN1) downregulation and ECM protein (COL1, FN1) upregulation paralleled the expression of nuclear NKX2-5 **(Fig 2A, B)**. These findings were confirmed by immunoflurescence. Synthetic cells, expressed nuclear NKX2-5, high levels of intracellular pro-collagen type I (ProCOL1) and FN1, but low levels of ACTA2 **(Fig 2C)**. Conversely, contractile cells, expressed little NKX2-5, ProCOL1 and FN1, but high levels of ACTA2, organized into distinct cytoplasmic myofilaments **(Fig 2C)**. Culturing the cells under conditions promoting the synthetic phenotype, resulted in substantial morphological changes. While cells with low expression of NKX2-5 remained mostly unchanged, those with higher nuclear NKX2-5 levels, also stained strongly for proCOL1 and the cells become larger with obvious nucleoli, suggesting increased levels of euchromatin **(Supplementary Fig 3)**. A shape change also became evident as NKX2-5 accumulated. Where initially the cells were flatter and more spread out suggesting increased matrix interaction, but gradually as nuclear NKX2-5 builds up they become thinner and spindle shaped, with multiple pseudopodia, an indication of increased motility **(supplementary Fig 4)**.

We further probed the role of NKX2-5 in promoting these changes in gene expression and function using RNA interference (siRNA) **(Fig 3A)**. Cells grown under conditions that favour the synthetic phenotype and expressing high levels of NKX2-5 were treated with either non-targeting siRNA (siCON – 250 nmol/L) or NKX2-5 specific siRNA (siNKX2-5 – 50nmol/L or

250nmol/L). Knockdown of NKX2-5 expression downregulated synthetic markers (COL1, CCN2, FN1) and up regulated contractile markers (MYH11, ACTA2, SMNT).

NKX2-5 knockdown altered contractile and synthetic VSMC morphology **(Fig 3B)**. Untreated VSMC and those treated with siCONTROL expressed high levels of nuclear NKX2-5, high levels of proCOL1 and lower levels of ACTA2 with disorganised cytoplasmic actin fibrils and pseudopodial protrusions, when cultured under synthetic conditions. However, knockdown of NKX2-5 (siNKX2-5) rescued the contractile phenotype, decreasing the levels of ProCOL1 and while increasing ACTA2 levels and organization.

Constitutive over-expression of NKX2-5 inhibits the upregulation of contractile markers and upregulates collagen.

Further evidence supporting a causative relationship between NKX2-5 and the contractile phenotype, was obtained by stably over-expressing NKX2-5 in an immortalized hPASMC cell line (iPASMC) **(Fig 4A)**. The expression of NKX2-5 in this system is much higher than physiological levels, to make the repression and suppression of NKX2-5 genes easier to observe. These cells recapitulate VSMC behaviour by upregulating contractile markers under serum deprivation (19). Under reduced serum conditions and at low confluence, iSMC expressed contractile markers (TAGLN, CNN1, ACTA2), but do not express detectable levels of COL1. They responded to TGFβ, in a dose-dependent fashion, by further upregulating the contractile markers and switching on COL1 expression, albeit at a very low level. Forced constitutive expression of NKX2-5 in these cells (iSMC-NKX) with a lentiviral vector, altered their behaviour dramatically. Expression of TAGLN, CNN1 and ACTA2 was effectively abolished in iSMC-NKX, while COL1 was strongly upregulated. The iSMC-NKX cells still responded to TGFβ, by increasing the expression of contractile markers and COL1, but the overall

expression of contractile markers, remained very low relative to the iSMC-control cells transduced with a control virus. COL1 expression in the iSMC-NKX on the other hand increased substantially and was much more responsive to TGFβ even at low concentrations. The clear implication is that NKX2-5, does not block TGFβ signalling. Instead, it exerts direct control on the overall expression level of the contractile markers and COL1, effectively overriding TGFβ signalling.

We were able to recapitulate these results in primary cells. We transiently expressed NKX2-5 with a lentiviral vector in primary HPASMC cells and cultured them in 10% or 1% serum for 7 days. **(Fig 4B)**. Cells treated with a control lentivirus (ShC), upregulated CNN1, TAGLN and ACTA2 under low serum conditions. In contrast, contractile maker expression, in cells treated with the NKX2-5 lentivirus, did not respond to serum deprivation. These results suggest that NKX2-5 exerts direct control on contractile marker expression that can override external signals.

NKX2-5 regulates contraction, migration and proliferation

We tested the function of NKX2-5 in the various cellular processes which characterise the VSMC phenotype. I*n vitro* assays were used to assess cell contraction, migration and proliferation in the presence or absence of NKX2-5.

A tensioning culture force monitor (23) was employed to measure the force exerted by VSMC on a three-dimensional collagen gel matrix, as a measure of cell contraction. Collagen gels were seeded with contractile or synthetic VSMC that had been treated either with siCONTROL or siNKX2-5 (**Fig 5A**) and the exerted force was measured continuously for 24 hours. As expected, we found no appreciable difference between contractile cells treated with siCONTROL and siNKX2-5, consistent with a lack of NKX2-5 expression (**Fig 5A, upper panel**).

In contrast, siCONTROL treated synthetic cells markedly lower force (less than 50%) on the matrix compared to siNKX2-5 treated synthetic or contractile cells (**Fig 5A, lower panel**). Thus NKX2-5 inhibition rescued the decreased contractility associated with the synthetic phenotype.

We also tested the migratory capacity of VSMC in the presence or absence of endogenous NKX2-5 using an *in vitro* scratch wound assay. After 48 hours, synthetic cells showed considerably greater migration than contractile cells. NKX2-5 knockdown significantly inhibited synthetic VSMC migration (**Fig 5B & 5C**). In contractile cells, siRNA treatment had no significant effect (data not shown).

Finally, we assessed the effect of NKX2-5 inhibition on VSMC proliferation. Using siNKX2-5 or siCONTROL oligonucleotides in synthetic VSMC, we measured proliferation rates over 48 hours. Once again siCONTROL treatment produced no significant difference compared to untreated, but siNKX2-5 reduced the proliferation rate in a dose-dependent fashion. (**Fig 5D**). These findings were confirmed in synthetic VSMC explanted from inducible knockout NKX2-5 (NKX2-5^{flox}Col1α2^{CreERT}) mice, and then exposed to adenovirus particles containing either Cre recombinase (Ad.CRE) or green fluorescent protein (GFP; control). The proliferation rate of cells lacking NKX2-5 was significantly decreased throughout the time course (**Fig 5E**).

Mechanism(s) of NKX2-5 activation in vascular smooth muscle cells

A biologically relevant level of NKX2-5 expression in hPASMC is observed only in synthetic conditions, i.e. 10% serum and low confluence. The process takes several days, but hypoxia and stimulation with exogenous TGFβ can accelerate it, resulting in NKX2-5 appearing earlier than it does with serum alone **(Fig 6A)**. NKX2-5 reactivation coincides with an increase of phosphorylated AKT. To delineate the NKX2-5 activation mechanism(s) in HPASMC, we

investigated signalling pathways downstream of TGFβ and hypoxia. Using specific inhibitors of the PI3K pathway (GSK2126458) **(Fig 6B and C)** and TGFβ receptor 1 (SD208) (**Fig 6D**), we determined that NKX2-5 expression in synthetic HPASMC is decreased when these pathways are inhibited. Similarly, specific inhibition of extracellular-signal-regulated kinase 5 (ERK5), a MAPK family member associated with cardiovascular development and stress stimuli, results in a significant decrease of NKX2-5 **(Fig 6B and C)**. Inhibition the TGFβ pathway also results in the inhibition of ERK5 phosphorylation to its active form **(Fig 6D)**. Other specific inhibitors for ASK-1 (TC ASK10, **Fig 6C and D**), TAK1 (MAPKKK, (5Z)-7-Oxozeaenol), p38 MAPK (SB202190), ERK1,2 (FR 180204), JNK (BI 78D3) did not have a significant impact on NKX2-5 expression (data not shown). We verified the ERK5 data using siRNA **(Fig 6E).** An 80% downregulation of ERK5, in cells cultured for 2 days with 10% serum and 0.5ng/mL TGFβ, resulted in a 25% reduction of NKX2-5 relative to cells treated with control siRNA. Our proposed mechanism of NKX2-5 activation in HPASMC involves the PI3K/AKT, TGFβ and ERK5 pathways **(Fig 6F)**. We propose that a combination of damage signals, such as hypoxia and the presence of serum combined with TGFβ signalling (either exogenous or autocrine) are needed to reactivate NKX2-5, via the PI3K and ERK5 pathways.

Targeted NKX2-5 deletion in the chronic hypoxia model of pulmonary arterial hypertension

Having determined, that NKX2-5 is a critical factor in VSMC phenotypic modulation and that hypoxia one of the main regulatory pathways, we sought to confirm this *in vivo*, using a hypoxia-induced mouse model of PAH. We used an NKX2-5 conditional deletion model, to prove that vascular remodelling requires the presence of NKX2-5. The condition for deleting NKX2-5 was activation of the COL1A2 enhancer, rather than the COL1A2 promoter. Although a wide variety of cells transcriptionally regulate expression of COL1A2 via the promoter,

activation of the COL1A2 enhancer is limited to a subset of mesenchymal cells, mostly fibroblasts. In vascular smooth muscle cells, the COL1A2 enhancer is activated only in cells undergoing de-differentiation towards a 'synthetic' phenotype driving the over-expression of collagen type I (18). Therefore, conditional deletion of genes using the COL1A2 enhancer to drive Cre recombinase, will only be achieved in vascular smooth muscle cells undergoing phenotypic switching to the 'synthetic' phenotype. 'Contractile' VSMC cells will not be affected, while for non-vascular cells that do not express NKX2-5, the deletion will have no impact. Cells such as cardiomyocytes, which express NKX2-5 but the COL1A2 enhancer is not activated, will not conditionally delete NKX2-5.This system ensures that the observed effects are directly attributable to deletion of NKX2-5 from VSMC.

Inducible conditional-null NKX2-5 mice were created by mating NKX2-5^{flox} mice (24) with collagen type Iα2 enhancer-driven CreERT mice. These transgenic mice contain the mesenchymal cell-specific enhancer of the mouse Col1α2 gene, driving the expression of a polypeptide consisting of a fusion between Cre recombinase and a mutant ligand-binding domain of the oestrogen receptor (25) **(Fig 7A)**. In these Col1α2 Cre-ERT–transgenic mice, administration of tamoxifen (4-OHT) activates Cre recombinase in cells where collagen type Iα2 is being over-expressed by VSMC, including in injured blood vessels. Polymerase chain reaction (PCR) assays using specific primers (P1-P2 and P1-P3) were used to confirm NKX2-5 deletion. NKX2-5 was knocked out in adult NKX2-5^{flox} Col1α2CreERT^{+} (NKX2-5^{flox} Cre^{+}) mice in remodelling vessels **(Fig 7A-D)** by 4-OHT administration for five consecutive days beginning on day 3 after the mice were placed in the hypoxic chamber. Collagen type Ia2 enhancer reporter mice were used to determine the optimum time point of activation of the Col1a2 enhancer by tamoxifen administration **(Supplementary Fig 5)**. Two groups of controls were used: NKX2-5^{flox} Cre^{+} mice injected with corn oil instead of tamoxifen ('NKX2-5^{flox} Cre^{+} Cornoil'), and NKX2-

5^{flox} Cre^{-} mice injected with tamoxifen ('NKX2-5^{flox} Cre^{-} 4OH-T'). The mice were sacrificed after 21 days under hypoxia. Parallel groups of mice treated identically were kept under normoxic conditions. Total RNA expression was measured using quantitative PCR (qPCR) (**Fig 7B**). Pulmonary arteries were analysed for NKX2-5 protein expression by western blotting (**Fig 7C**). Finally, immunohistochemistry for NKX2-5 was performed on lung sections from these mice (**Fig 7D**). NKX2-5 was not detectable by any of these methods in pulmonary vessels under normoxic conditions; it was elevated in both the hypoxic control mouse groups but was not detectable in NKX2-5 null mice under hypoxic conditions.

NKX2-5 deletion inhibits vascular remodelling and decreases pulmonary vascular resistance

Medial thickening is one of the characteristics of pulmonary arterial remodelling. This is driven by the expansion of the VSMC layer. The major source of new VSMCs results from the process of phenotypic modulation. The VSMC expansion leads to increased artery muscularization, stronger vascular tone and narrowing of the vessel lumen. We expect that deletion of NKX2-5 will block this process by preventing VSMC from switching to the synthetic phenotype and proliferating. We also expect that NKX2-5 deletion will leave ACTA2 staining unchanged as expansion of the VSMC layer will be prevented. In contrast in the WT mouse where NKX2-5 can be reactivated, increased muscularization will lead to the appearance of a thicker more densely stained VSMC layer. Muscularization of small (20-50μm diameter), medium (40-70μm) and large (>70μm) arteries occurred after 21 days under hypoxic conditions in both control mouse groups. The NKX2-5-null mice under hypoxic conditions showed significantly less vascular muscularisation ($p<0.001$) in small, medium and large vessels, so that they resembled the pulmonary vessels of mice kept under normoxic conditions (**Fig 8A and B**). After 21 days of hypoxia the mice were anaesthetised, and the

right ventricular systolic pressures (RVSP) were measured using a catheter. Under normoxic conditions the mean RVSP was 20 ± 1.4 mmHg. After hypoxia the RVSP in the NKX2-5^{flox} Cre^{+} Cornoil and NKX2-5^{flox} Cre^{-} 4OH-T control groups were elevated to 40.2 ±2.4 mmHg and 37.6 ± 1.8 mmHg respectively. However, the RVSP of the NKX2-5-null group was significantly lower (29.2 ± 2.3 mmHg; $p<0.01$: **Fig 8C)**. There were no differences in mean arterial blood pressure between the groups (data not shown).

The impact of NKX2-5 deletion on vessel compliance was measured using myography on first- and second-order pulmonary arteries removed after the RVSP measurements had been taken. A small vessel wire myograph was used to study contraction and relaxation responses in terms of changes in isometric tension development **(Fig 8D)**. Phenylephrine (PE; 1 nmol/L-5 µmol/L) was used to induce vasoconstriction, and the nitric oxide donor sodium nitroprusside (SNP; 1 nmol/L-10 µmol/L) was used to induce relaxation. The contraction response curves of vessels from NKX2-5 null mice were shifted to the left compared to controls, showing that the vessels were more sensitive to PE. Similarly, vessels from NKX2-5 null mice were more sensitive to the relaxing effects of nitric oxide (**Fig 8D**).

Right ventricular (RV) hypertrophy is a well described characteristic of the chronic hypoxia model of PAH. Conditional NKX2-5 deletion after 21 days of hypoxia reduced RV hypertrophy, as shown by a significant decrease in the RV/LV wet weight ratio (**Fig 8E**) and the absolute wet weights of the right ventricles alone. There were no physiologically relevant changes in left ventricle wet weight across the groups (data not shown). We tested whether this decrease was a direct result of the deletion of NKX2-5 from the cardiac tissues or an indirect consequence of the pulmonary changes described above. Analysis of NKX2-5 protein expression in the heart by SDS-PAGE and western blot revealed no perceptible differences between groups, suggesting that NKX2-5 was not deleted in the heart (**Fig 8F**). Using a

reporter gene driven by the COL1A2 enhancer, we showed that NKX2-5 in the heart is not deleted because the COL1A2 enhancer is not activated in cardiomyocytes, even under hypoxic conditions, so Cre recombinase is not expressed **(Supplementary Fig 5).** As a measure of ECM production, we analysed collagen type I expression in lungs from NKX2-5 null and control groups. We found significantly lower levels of collagen type I in the NKX2-5 null mouse lungs **(Supplementary Fig 6),** confirming the role of NKX2-5 in ECM deposition.

Discussion

Vascular remodelling a pathophysiological manifestation of many diseases such as atherosclerosis, peripheral artery disease, hypertension, pulmonary hypertension, and restenosis after angioplasty. It is an adaptive response to injury, inflammation, changes in blood flow, tensile stress and shear stress (26,27). Vascular remodelling requires VSMC proliferation, which in turn requires that some of the VSMC switch to the synthetic phenotype. Over time this expansion of the VSMC population drives thickening of the vessel wall. In this study we provide multiple lines of evidence demonstrating that NKX2-5 is a powerful modulator of the VSMC phenotypic switch.

We prove conclusively that in cultured HPASMC, the synthetic phenotype requires NKX2-5. Key phenotypic determinants such as components of the contractile machinery, migration, proliferation and ECM production, are regulated by NKX2-5. Knockdown or forced overexpression of NKX2-5 abrogates VSMC phenotypic plasticity, locking them into the contractile or synthetic phenotype respectively.

The role of TGFβ in vascular remodelling and fibrosis is paradoxical. There is strong data implicating TGFβ activity in both normal function and disease. Studies like Chen et al (13), offer strong evidence that TGFβ is vital for normal healthy VSMC contractile function, but other studies offer equally strong evidence that TGFβ superfamily signalling promotes disease (28-29). A particularly salient example is the BMP receptor mutation in idiopathic pulmonary hypertension, which activates TGFβ signalling (30).

Our data are fully consistent with both observations and help unify the field. We show that NKX2-5 expression directly overrides the effects of TGFβ on VSMC phenotype by shutting down the expression of contractile genes and upregulating collagen, without blocking TGFβ signalling. Furthermore, we find that that TGFβ can contribute to NKX2-5 expression *in vitro*. We propose that when NKX2-5 expression is reactivated due to the combined effect of various upstream signals, it exerts a suppressive effect on the expression of the contractile gene set, antagonizing their upregulation by other pathways, including TGFβ. Both the contractile machinery and the matrix proteins in the synthetic set are TGFβ responsive, but normally TGFβ only promotes the contractile phenotype, because without NKX2-5 the synthetic genes are repressed. In the presence of injury or repair signals however, TGFβ helps reactivate NKX2-5, which in turn lifts the repression of the synthetic gene set, while attenuating the expression of contractile genes. TGFβ can thus promote either the contractile or the synthetic phenotype depending on whether NKX2-5 is also expressed.

A new report by Chen et al (31) investigating the role of TGFβ deletion in aortic aneurysms supports our proposal. The authors found that when the mice are exposed to atherosclerotic conditions after conditional deletion of the TGFBR2, aortic aneurysms can readily be

detected, due to loss of the smooth muscle phenotype. The authors proposed that vascular injury signals in the absence of TGFBR2 signalling result in activation of KLF4 signalling unchecked by SMAD2/3 repression, which in turn, reverts VSMC back to a mesenchymal stem cell-like phenotype. Thus, signals like vascular injury which promote the synthetic phenotype lead to VSMC de-differentiation in the absence of sufficient TGFβ signalling, demonstrating that TGFβ is needed for both the contractile and the synthetic phenotype.

Our data shows for the first time that ultimately the phenotypically plasticity of SMCs is controlled by underlying differentiation-regulating transcription factors such as NKX2-5, which then define the exact function of the overlying signalling pathways that regulate vascular function (e.g. TGFβ), drawing a parallel with phenotypic plasticity observed in immune cells. Therefore, we believe that NKX2-5 is not controlled by a single pathway but is rather a focal point for signalling arising from conditions associated with damage and inflammation. Our hypothesis explains why TGFβ and other members of the TGFβ superfamily can paradoxically contribute to pathogenesis in vascular disease, despite also being essential for normal vascular function.

Our studies of cell signalling underlying NKX2-5 activation in VSMC revealed that NKX2-5 induction by hypoxia, serum and growth factor stimulation proceeds via at least two signalling cascades: PI3K and ERK5. The PI3K pathway is directly related to the regulation of cell cycle (32) and proliferation and the ERK5 pathway is associated with cardiovascular development (33) and vascular differentiation programmes (34). Yet these two pathways are downstream of many different growth factors, including the TGFβ superfamily, PDGF, FGF and VEGF, which have both important homeostatic functions and are also involved in blood vessel response to

injury. This is consistent with our proposal that input for multiple pathways can induce the 'synthetic' phenotype and proliferation by helping upregulate NKX2-5 beyond a threshold level.

We confirmed this hypothesis using samples from patients with PAH. We robustly document for the first time, reactivation of NKX2-5 in damaged or diseased vascular tissue, where in control, healthy samples it is absent. We used a well-defined animal model that deletes NKX2-5 expression whenever the COL1A2 enhancer is activated. In adult VSMC cells, the COL1A2 enhancer is inactive under normal conditions. Vascular cells, however, do switch on the COL1A2 enhancer when they reactivate NKX2-5, under disease conditions. This system will therefore delete the NKX2-5 gene specifically in vascular cells, which have switched on NKX2-5 expression and in mesenchymal cells that do not actually express NKX2-5. As a result, NKX2-5 function will be specifically and selectively ablated only in vascular cells undergoing either phenotypic modulation to the synthetic phenotype or endothelial to mesenchymal transition, while leaving NKX2-5 in the heart intact (confirmed in fig 8F and suppl fig 5). Activated fibroblasts also activate the COL1A2 enhancer, but in our hands, we have been unable to detect NKX2-5 expression in lung fibroblasts under any conditions, nor were we able to observe NKX2-5 expression in the connective tissue of diseased lungs, human or murine (Figs 1, 7, and 8). Indeed, the current consensus in the field is that NKX2-5 is heart limited after development. Thus our system will only delete NKX2-5 either in synthetic VSMC or in mesenchymal cells that do not express NKX2-5 in the first place. NKX2-5 deletion in this fashion profoundly slowed the progression of vascular disease and inhibited pathological changes in mice subjected to chronic hypoxia. Without NKX2-5 any pathology related to the synthetic SMC phenotype is greatly attenuated or absent.

We sought further confirmation of our hypothesis that vascular injury and TGFβ superfamily signalling combine to reactivate NKX2-5, using the TGFβR2-kinase deficient model, which recapitulates key pathological features of systemic sclerosis (35-37). In this model, fibroblast specific expression of a dominant negative, kinase-deficient TGFβR2 variant, paradoxically results in constitutive overexpression of TGFβ1 ligand and strongly increased basal TGFβ superfamily signalling, leading to spontaneous development of fibrosis and PAH with age. Previous work by our group, revealed that in young mice, before overt PAH and fibrosis develops, increased thickness to circumference ratio is already present and SU5416 vascular injury, rapidly precipitates a strong increase in RSVP. We obtained lung sections from transgenic mice with or without SU5416 treatment and the WT controls (kindly donated by Dr Derrett and prof Denton, Centre for Rheumatology and Connective Tissue Diseases, University College London) and stained them for NKX2-5 **(supplementary fig. 7)**, revealing that NKX2-5 is indeed reactivated in the transgenic mice and its expression further increased by SU5416. This is as predicted by our proposed model **(fig 6F)** that stipulated cooperative activation of NKX2-5 by repair signals stemming from vascular injury and TGFβ superfamily signalling. We have thus shown that vascular remodelling is associated with unexpected NKX2-5 reactivation in vascular cells, in three separate settings: *In vitro* in HPASMC and in two separate, established *in vivo* models of PAH, one driven by hypoxia and the other driven by TGFβ superfamily signalling and vascular injury.

It should be noted that we have left one potentially important signalling component unexplored in this work, namely mechanosensing. In Dritsoula et al (19), we demonstrated that YAP binds the NKX2-5 promoter/enhancer. Given the pivotal role of YAP in mechanical signal transduction, this suggests that NKX2-5 is a mechanosensitive gene. The obvious

implication is that increased mechanical load may be an independent driver of NKX2-5 reactivation and thus in addition to vascular repair, NKX2-5 may also be involved in maladaptive responses to mechanical stimuli.

A very relevant recent report (38) found that NEDD9 an important scaffolding protein, which can associate with both SMAD3 and NKX2-5, has its target preference regulated by oxidative stress and hypoxia among other signals, but is independent of TGFβ signalling. Under oxidative stress in pulmonary endothelial and smooth muscle cells, association with SMAD3 is discouraged and association with NKX2-5 is encouraged, enhancing NKX2-5 activity. This report offers evidence of an alternative pathway leading from hypoxia and oxidative stress to post-translational NKX2-5 activation, thus corroborating our hypothesis that multiple signals converge on NKX2-5. The authors also show that pulmonary hypertension and vascular fibrosis are attenuated by inhibition of NEDD9, further confirming our findings that NKX2-5 is a critical regulator of vascular remodelling.

Our study offers an exciting new insight into VSMC phenotypic modulation. During embryonic development vascular cell progenitors are freely able to proliferate as part of the vascular ontogenesis programme, but mature differentiated cells in the adult vessels lose this ability. NKX2-5 follows the same pattern. It has an essential role in directing embryonic vessel formation (39), but its expression is shut down in adult vessels. We found that NKX2-5 can be reactivated in adult vessels to partially recapitulate the embryonic differentiation programme, enabling vascular repair and regeneration. Thus, phenotypic modulation, does not reflect a permanent and pathologic de-differentiation of vascular cells, but rather a temporary re-

activation of proliferation as part of the normal vascular repair process. It is pathogenic only when it becomes chronic and dysregulated.

Typically, tightly regulated developmental pathways are regulated by a combination of positive and negative control. Examples include polycomb (PcG) and Trithorax (TrxG) (40), Groucho and TCF (41), Sonic Hedgehog (SHH) and Gli3 (42). We have already documented NKX2-5 acting through competition with the repressor ZEB in the regulation of Collagen type 1 expression in SMC (18). We expect that a counterpart for NKX2-5, suppressing the synthetic phenotype also exists and controls VMSC plasticity together with NKX2-5. Other transcription factors implicated in VSMC phenotypic modulation such as SRF, KLF4, myocardin and ZEB are all functionally linked to NKX2-5 (18,43-47).

We believe that this role of NKX2-5 in repair can be effectively exploited therapeutically. Although inhibition of NKX2-5 in healthy vessels could potentially block vital repair pathways, when NKX2-5 reactivation has already become pathological such as pulmonary hypertension and atherosclerosis or following angioplasty and stenting it may be very beneficial. Furthermore, NKX2.5 may be a critical factor in applications seeking to exploit ex-vivo angiogenesis.

Recently, a study (46) using lentiviral induction of NKX2-5 in vivo suggested a protective role for *transient* endothelial NKX2-5 expression in atherosclerosis. After careful reflection, we concluded that this report does not contradict our findings. The authors injected the lentivirus in the blood stream of mice on an atherogenic diet and followed the mice over 21 days. This will result in temporary expression of NKX2-5 in the endothelium and not the underlying

VSMC layer. The authors confirmed that forced expression of NKX2-5 in the endothelium did nor persist. Yet, the authors also detect NKX2-5 expression in the smooth muscle cells specifically in the atherosclerotic lesions, directly corroborating our findings. This expression is not due to transduction, but due to the damage caused to the vasculature. Unfortunately, they only investigate the effect of NKX2-5 overexpression in smooth muscle cells cultured under conditions promoting the synthetic/proliferative phenotype, without a comparison with cells in the contractile phenotype, so they do observe not observe any phenotypic changes because they have already made the cells synthetic. Their observation of an atheroprotective effect after transient endothelial NKX2-5 expression is consistent with the repair role we have proposed and it is also consistent with the finding by Deng et al (48) that MEKK3/ERK5 deletion in endothelial cells can promote arterial remodelling. Our model suggests that a temporary, acute induction of NKX2-5 early on during injury, will be beneficial by promoting repair, yet without persisting long enough to induce disordered proliferation and vascular dysfunction. Ultimately this report supports, rather than contradicts, our finding that NKX2-5 is essential for vascular repair, and it is only chronic, persistent expression that is pathologic. Crucially, the authors have independently confirmed NKX2-5 reactivation in the vasculature under disease conditions.

In summary, we have conclusively demonstrated for the first time a role for NKX2-5 expression in human vascular pathology. We showed that NKX2-5 regulates VSMC phenotypic modulation, and that its expression results in VSMC proliferation, migration, inhibition of the cellular contractile apparatus, and modulation of the ECM. We propose that NKX2-5 is part of the vascular repair process, but chronic expression promotes vascular remodelling.

Methods

Sex as a biological variable

The human samples originated from donors of both sexes. For the mouse experiments only males were used, to avoid potential interference arising from the oestrogenic activity of tamoxifen. Although there are known sex differences in hypertension and scleroderma in general, we do not consider sex as an important biological variable in this study. This is because in our in vitro experiments we didn't observe any material differences between cells from male and female donors with respect to the function of NKX2-5 in regulating smooth muscle phenotypic modulation.

Human Tissue

Pulmonary tissue from patients in our scleroderma cohorts with pulmonary arterial hypertension, as well as healthy and atherosclerotic aortas (supplemental fig 2) and coronary arteries (supplemental fig 2) were obtained post-mortem. Carotid tissue (supplemental fig 2) was obtained after carotid endarterectomy and femoral arteries (supplemental fig 2) were obtained from amputations after Chronic Limb Ischemia.

Mice

To generate NKX2-5 deficient mice, we obtained mice homozygous for the *NKX2-5floxed* allele (a generous gift from Prof Pashmforoush Keck school of Medicine, University of South California) previously described in Pashmforoush et al (24). Mice homozygous for the 'floxed' NKX2-5 allele were crossed with Col1a2CreERT mice (49) to generate conditionally induced NKX2-5 knockout mice in cells that have an activated Col1a2 enhancer element and are therefore overexpressing collagen type I. Col1α2CreERT transgenic mice carry a tamoxifen inducible Cre recombinase element under the control of the enhancer/promoter sequence of the pro α2(I) collagen gene. 4-hydroxy-Tamoxifen (4OH-T) induction was carried out either by

intra-peritoneal injection for five consecutive days or included in the normal rodent diet at a concentration of 400mg/kg (Harlan) and administered throughout the duration of the experiment (50,51). All mice used in this study are derived from 129 and crossed into C57BL/6 background and only male mice were used. Genotyping was performed by PCR analysis of tail DNA using Cre-specific primers and primers that spanned intron 1 and exon 2 of NKX2-5 gene. The somatic deletion of NKX2-5 in pulmonary arterial smooth muscle cells after 4OH-T administration was confirmed with PCR using three primers CAAATCTTCGTACTGGAGAGT (P1), CCTGCCTGGAGATTGTACTAGAA (P2) and TGAGCTGAATACATCCCCTAGTTG (P3). The P1-P2 primer pair produces two different products with the wild type (490bp) and floxed allele (630bp). The P1-P3 only produces a product with the cre-deleted floxed allele (~700bp). The PCR reactions were carried out using the fast-cycling PCR kit (QIAGEN), with a 57^{o}C annealing temperature and 1 µM primer concentration.

To characterise Col1a2 enhancer activity within our injury models, we used the collagen type Ia2 enhancer reporter mouse (Col1a2-LacZ-Tg) which was previously described and characterised (18). All studies conformed to the UK Animals (Scientific Procedures) Act 1986.

Chronic Hypoxia Mouse model of PAH: Mice (12-week-old male mice, 20–25 g) undergoing exposure to hypoxic conditions were housed in a normobaric hypoxia chamber (850-NBB Nitrogen Dry Box; Plas-Labs) for 3 weeks. Room air balanced with N_2 achieved an FiO_2 value of 0.10. CO_2-absorbent lime was added to maintain the CO_2 content at <1.0%. Gas tension and humidity values were determined daily to ensure optimal conditions. Mice placed in the hypoxic chamber and administered with 4-hydroxy-Tamoxifen (4OH-T) by intra-peritoneal injection for 5 consecutive days starting at day 3. At day 21 the right ventricular systolic pressure was measured, and the mice were sacrificed. The mice were anesthetized with 1.5% isoflurane and placed in a supine position onto a heating blanket that was thermostatically

controlled at 37°C. Firstly, the right jugular vein was isolated, and a Millar SPR-671NR mouse pressure catheter with a diameter of 1.4F was introduced and advanced into the right ventricle to determine RVSP. The mean arterial blood pressure (MABP) was also measured by isolating the left common carotid artery and introducing a pressure catheter. Both RVSP and MABP measurements were recorded into a pre-calibrated PowerLab System (ADInstruments). The mice were killed by isoflurane aesthetic overdose, whole blood samples and lungs were collected, the hearts were removed, and the weights of the right and left ventricles were recorded. Right ventricular hypertrophy was determined and expressed as the weight of the right ventricle to left ventricle plus septum ratio; RV/LV+S. The left lung was then fixed by inflation with 10% formalin in PBS before paraffin embedding and sectioning. The remaining lung tissue, heart, and kidney were dissected and snap frozen in liquid N_2. Plasma was collected by centrifugation and stored at −80°C.

Morphologic analysis: Transverse formalin-fixed lung sections were immunostained using a specific antibody for a-smooth muscle actin (Acta2). Pulmonary arterial muscularisation was expressed as the thickness to circumference ratio. Briefly, vessels of between 20-100 µm in diameter were imaged in each group of mice. At least a total of 300-500 vessels per group were quantified.

Myography: Mouse lungs were removed from freshly sacrificed mice into cold (4°C) physiologic salt solution. Under light microscopy, second and third-order pulmonary arterial branches (internal diameter, ~200 µm) were dissected, and 2-mm-long segments were mounted in a dual-chamber wire myograph (model 510A, Danish MyoTechnology, Aarhus, Denmark) for isometric tension recording. Vessels were bathed in 10 mL of physiologic salt solution, heated to 37°C, and bubbled continuously with 95% oxygen/5% $CO_2$and stretched to 90% of the diameter achieved when under a transmural pressure of 15 mm Hg. After 30 mins

of equilibration, an automated normalization procedure was performed to determine the arterial lumen necessary for optimal force generation. Vessels were pre-contracted using the thromboxane-A_2 analogue (U46619, 100nM), 30 minutes after normalization. Endothelial integrity was confirmed by demonstrating a >=50% relaxation to 10 µM acetylcholine applied at the peak of contraction. Concentration-response curves for contraction to phenylephrine (PE; 10^{-9} to 10^{-4}M) or relaxation in response to sodium nitroprusside (SNP; 10^{-9} to 10^{-4} M) were constructed.

Vascular Smooth muscle cell culture

In vitro phenotypic modulation: Vascular smooth muscle cells were cultured using a protocol adapted from one previously described (52). Commercially obtained human VSMC (C-12521, Promocell) were grown from passage 2 in VSMC-specific Medium (Promocell) to confluence. The post-confluent cells were maintained in VSMC medium with 10% foetal bovine serum, passaging them when they reach 60% confluence. These conditions favour the synthetic /proliferative phenotype. To induce contractile gene expression the VSMC were seeded at high density (above 70% confluence) in VSMC specific medium containing 1-4% serum, depending on the application (see main text). An immortalized cell line derived from primary human pulmonary VSMC (iSMC – T0558, ABM Good), was cultured in the same way.

Adenoviral transduction: Explanted mouse aortic SMC were grown in T25 flasks (Corning Inc., Corning, NY, USA) to 70% confluence then transduced at an moi of 100 with either Ad.CRE (Ad5 serotype adenovirus expressing CRE recombinase from the CMV promoter) or Ad.gfp (Ad5 serotype adenovirus expressing green fluorescent protein from the CMV promoter, negative control). Briefly, the cell monolayer was washed in phosphate buffered saline (PBS) to remove all serum, incubated for 2hrs with adenoviral particles in a minimal volume of

medium without serum, washed twice in PBS to remove any remaining virus particles, then normal growth media was replaced. After viral transduction the cells were allowed to recover for 24hrs.

Lentiviral transduction: Lentivirus vectors were produced in HEK293T (CRL11268, ATCC) using the psPAX2 (#12260, AddGene) and pMD2.G (#12259 Addgene) packaging plasmids. The vector genome was provided by either pLenti-GIII-CMV-GFP-2A-Puro (ABM Cat#318840610395) or the SMARTvector Inducible Lentiviral shRNA plasmid (#V35H11252, Dharmacon). The plasmids in a genome:capsid:env ratio of 4:3:1 were transfected into HEK293T cells using the FuGene HD transfection reagent (Promega), using 0.5µg/cm2 of culture area, according to the manufacturer's instructions. The lipid complexes were formed in Opti-MEM I (Thermofisher). At 24h post-transfection the media was changed to fresh growth media with 0.1% BSA. The supernatant was harvested every 24h for 72h. Immediately after each harvest, the media was passed through a 0.45 µm PES filter aliquoted and snap frozen. VSMC at 80% confluence were infected using 0.1mL of crude viral supernatant per cm2 of culture area for 6h, twice on consecutive days. The transduced cells were selected with 1µg/mL puromycin for 3-5 days. Prior to use the cells were allowed 24h in growth media without puromucin.

RNA interference: Human VSMCs were grown under conditions which favoured either the contractile or the synthetic phenotype, then preincubated in OptiMEM I for 3 hours and transfected with 10 nM small interfering RNA [siRNA; Dharmacon NKX2-5 siGenome Smartpool (siNKX2-5)] or Dharmacon scrambled control siRNA [siCONTROL (siCON)] using Oligofectamine^{TM} transfection reagent (InVitrogen). The cells were used in contraction, migration proliferation assays.

Contraction: Measurement of contractile force generated within a three-dimensional, tethered floating cell-populated collagen lattice was performed as described previously (18,51). Briefly using 1 × 10^6 cells/ml of collagen gel (First Link, Birmingham, USA), we measured the force generated across the collagen lattice with a culture force monitor (CFM). This instrument measures the minute forces exerted by the HASMC within a collagen lattice over 24 hours. In brief, a rectangular smooth muscle cell seeded collagen gel was cast and floated in medium. The collagen gels were tethered to two flotation bars on either side of the long edges, and, in turn attached to a ground point at one end and a force transducer at the other. Cell-generated tensional forces in the collagen gel were detected by the force transducer and logged into a personal computer. Graphical readings were produced every 15 s providing a continuous measurement of force generated.

Migration assay: Contractile and synthetic VSMC were seeded on plastic in the presence of anti-proliferative mitomycin C and treated with either siCONTROL or siNKX2-5 (Dharmacon). Briefly, a scratch wound was made across the plate to remove the cells using a device which allows all the scratches to be identical in dimensions. The cells were allowed to migrate into the wound and after 48 hours the percentage cell migration per 1$mm^2$are was measured as described in (18).

Cell proliferation assay: Human and mouse VSMCs were plated at a density of 15,000 cells per well in 24-well plates and then serum-starved for a further 24 h. The cells were trypsinized and counted using trypan blue (Sigma) exclusion for *0, 12, 24, 48*, and *72 hours* (*n* = 4 wells per treatment) and number of viable cells was determined. Each isolate was studied at least twice under each condition, and the mean values were taken from all studies conducted with any one isolate.

Histology, Immunohistochemistry and Immunofluorescence and Image analysis, Western Blotting

Antibodies: Several different NKX2-5 antibodies were validated and used over the course of each study: sc-14033, sc-12514 (Santa-Cruz Biotechnology), ab54557, ab35842 (Abcam) and E1Y8H #8792 (Cell Signalling Technology). Other antibodies used were: ACTA2 (C6189 and A5691 – Merck, US and M0851 – Agilent US), MYH11 (ab682, Abcam, UK), SMTN (sc-28562, Santa-Cruz Biotechnology), TAGLN (ab28811 and ab14106, Abcam, UK), Collagen type I (ab34710, Abcam, UK), Calponin CNN1 (17819s, Cell Signalling Technologies, US) intracellular procollagen type I (ab64409, Abcam, UK), Connective Tissue Growth Factor CTGF/CCN2 (sc-14939, Santa-Cruz Biotechnology), fibronectin FN1 (610078 BD Biosciences), and GAPDH (ab8245, Abcam, UK), Tata-Binding Protein, TBP (8515, Cell Signaling Technologies, US). In addition, antibodies for phospho-Smad3 (9520, Cell Signalling Technology), phospho Smad2/3 (ab276140, abcam), Erk5 (3372S, Cell Signalling Technology) and phosphoERK5 (3371, Cell Signalling Technology), AKT (#9272, Cell Signalling Technology) and phosphoAKT (Ser473) (9271, Cell Signalling Technology) were used.

Patient tissue samples: Tissue samples were obtained post-mortem from patients in our scleroderma cohort, who had a confirmed PAH diagnosis, defined at right heart catheterisation, by a mean pulmonary arterial pressure of 25mm Hg or greater.

Histology: Tissue samples were formalin-fixed, paraffin-embedded and sections (3–5 μm) were cut. Tissue architecture, non-fibrillar collagen, extracellular matrix and elastin were determined using standard staining protocols for hematoxylin and eosin (H&E), Masson's trichrome (MT) staining elastic–van Gieson (EVG) and picrosirius red (PSR). The birefringence of PSR staining visualised under polarised light filters is highly specific for collagen where the

larger collagen fibers are bright yellow or orange, and the thinner ones, or newer fibres, are green.

Immunohistochemistry: Immunohistochemistry was performed on formalin fixed paraffin-embedded tissue. Endogenous peroxidase was blocked using 3% hydrogen peroxide. Optimally diluted antibodies were used at appropriate concentrations. Specificity of staining was confirmed using isotype-matched IgG control antibodies. NKX2-5 staining was visualized by DAB and ACTA2 staining was visualized by Vector Red Alkaline Phosphatase Substrate kit (Vector Laboratories), and sections were counterstained by hematoxylin. Sections were examined with an Axioskop Z bright field microscope (Carl Zeiss, Germany) using Axiovision software.

Immunofluorescence: Cells were seeded for staining in chamber slides (BD Bioscience), fixed with cold methanol or 4% paraformaldehyde (PAF), and permeabilized with 0.2% Triton in phosphate buffered saline before blocking with isotype-matched serum for 30 minutes. The cells were then stained for 1 hour with various antibodies at 1:100 dilution, washed, and incubated with the appropriate conjugated secondary antibody (Vector BioLabs) before mounting with Vectastain containing DAPI, and examined with an Axioskop Z Fluorescence Microscope (Zeiss). Z-stacking and deconvolution protocols were applied to images of cells to determine nuclear localization.

Western Blotting: NuPAGE Bis-Tris kits (GE healthcare), were used according to the manufacturer's instructions. MOPS running buffer and Nitrocellulose membranes (Hybond-C; GE healthcare) were used for blotting. Protein bands were visualised using chemiluminescence with HRP linked secondary antibodies (GE healthcare) and photographic film (Hyperfilm ECL; GE healthcare).

RNA isolation and quantitative RT-PCR analysis

VSMC were lysed in 1 mL Qiazol, mixed with 200 uL chloroform, centrifuged at 13,000 rpm at 4°C, and the aqueous phase was transferred to fresh tubes and mixed with 1.5 volumes of absolute ethanol. This was then transferred to RNeasy spin columns (Qiagen, UK) and RNA was purified according to the manufacturer's instructions. RNA purity and quantity was determined using a NanoDrop spectrophotometer and integrity was determined by capillary electrophoresis (Agilent Bioanalyzer, UK). Samples were used if $A_{260/280}$ >1.98 and RIN > 9.5. 1 ug of RNA was reversed-transcribed using a Quantitect reverse transcription kit, including a gDNA wipeout step and RT negative controls for each sample. All primers spanned an intron and potential secondary structure was excluded by M-fold. cDNA was amplified using a Sensimix No SYBR greenPCR kit using a Rotor-Gene 6000 (Corbett Research, UK) and melt curves were checked for product specificity. Standards, 10^7-10^1 copies uL^{-1}, were also prepared from VSMC cDNA purified by agarose gel extraction (Qiagen, UK) and were included in each run, as were no-template controls to exclude template contamination, and for two reference genes (ACTB or SDHA), RT negative controls to exclude gDNA contamination. Assay efficiency was determined from the standard curves, which were used to derive copy numbers. Assay specificity was confirmed by BLAST, a single peak on melt curves, a single band on agarose gel and product sequencing. A panel of six reference genes was initially used to select the most stable genes for data normalisation using geNorm (53). The primer sequences for the human genes of interest written 5'-3'were as follows: NKX2-5, forward GGACCCTAGAGCCGAAAA and reverse CCGCTCCAGCTCATAGA; COL1A2, forward GCACATGCCGTGACTTGAGA and reverse GGATTAGTTCCTACGTGATACCTAC; ACTA2, forward GGAATCCTGTGAAGCAGCTC and reverse CCGATCCACACGGAGTA; TAGLN forward GATTCTGAGCAAGCTGGTGA and reverse TCTGCTTGAAGACCATGGAG; CCN2

GCTGACCTGGAAGAGAACATTA and reverse GCTCGGTATGTCTTCATGCT; SDHA forward AGAAGCCCTTTGAGGAGCA and reverse CGATCACGGGTCTATATTCCAGA; ACTB forward CACCATGTACCCTGGCATT and reverse CCGATCCACACGGAGTA.

Mouse sample protein analysis

Mouse tissues (pulmonary, vascular and heart) were dissected to isolate VSMC which were then homogenized and lysed. The lysates were either stored at −80°C or analysed by western blotting as described above.

Inhibitor treatment

Immortalised human pulmonary artery smooth muscle cells (ABM) were grown on collagen coated flasks in DMEM supplemented with 5% serum. The cells were plated to 60%-70% confluence and serum-starved then treated with 2ng/ml TGFβ (R&D, 240-B-010) for 24 hours. After TGFβ treatment, the cells were placed in 5%FBS/DMEM and the inhibitors were added as follows: TCASK10 (Tocris, 4825) at 10μM, ERK5-in-1 (Selleckchem, S7344) at 5μM, GSK2126458 (Selleckchem, S2658) at 3μM. The cells were treated with the inhibitors for 24 hours before harvesting for protein and RNA. Western blot assays were used to assess the levels of the proteins using the following antibodies: NKX2-5 (ab54567) and GAPDH (ab8245) from Abcam; AKT (9272), P-AKT (9271), ERK5 (3372), P-ERK5 (3371), P-SMAD2 (3101), P-SMAD3 (9520) (all from Cell Signalling). Images were analysed using ImageJ (NIH,USA).

Statistical analysis

Data are presented as means ± s.e.m. Unpaired t-tests were used for comparison between two groups, and two-way analysis of variance (ANOVA) used for comparison among groups. Values of $P<0.05$ were considered as significant. Data obtained from the two-way factorial design were analysed with two-way ANOVA. For *in vivo* studies, changes in MABP, RVSP,

RV/LV ratio, and muscularization of arteries were analyzed by one-way ANOVA. Results are expressed as mean ± SEM, and $P < 0.05$ denotes significance. Neointimal/lumenal areas of remodelled vessels and concentration/response curves were fitted to all the data using nonlinear regression and the –log [M] and analyzed using two-way analysis of variance (ANOVA) and $P < 0.05$ was taken as statistically significant. (GraphPad Software, San Diego, CA). For densitometry analysis of western blot, where there three or fewer comparisons to be made statistical significance was assessed with paired two tailed t-tests. For a single comparison the significance threshold was set to 0.05, while for two or three comparisons the significance threshold was set to 0.01 to control the false discovery rate. For experiments with a large number of comparisons, such as figure 2, 3 and 4, ANOVA analysis was used with post-hoc t-tests to confirm key results. Since several genes are being examined and we expect that their behaviour should be coordinated, in lieu of multiple testing adjustments we impose the stronger condition that differences in all linked genes should be significant at the $P<0.05$ level in order to reject the null hypothesis. The results of the ANOVA analysis for figures 2, 3, 4 can be found in supplementary figures 8, 9 and 10 respectively.

Study approval: All human tissue used in this study was obtained with consent for research purposes and approved by the Royal Free and Medical School local Research Ethics Committee. All animal measurements were carried out under Home Office animal licence No PPL- 70/8050. Strict adherence to institutional guidelines was practiced, and local ethics committee and Home Office approval were obtained prior to all animal procedures.

Data availability:

The raw data used to make the graphs found in the manuscript's figures are available in the accompanying "Supporting data values" excel spreadsheet file.

Author contributions: IP – experimental design, experimental work, data acquisition, data processing, writing the manuscript. AD, PK, RB, ST, EC, XS and AH – experimental work, data acquisition, data processing. CPD, DJA – experimental design, providing reagents, manuscript editing. MP - experimental design, experimental work, data acquisition, data processing, writing the manuscript, editing the manuscript.

Acknowledgments: We thank Prof M. Pashmafaroush for providing the floxed NKX2-5 mice. We also thank Dr Derrett-Smith for contributing the TGFβR2Δk transgenic mouse lung tissue. This work was supported by grants from the British Heart Foundation FS/05/062 (to M.P.) and Arthritis Research UK (now Versus Arthritis) 19427 and 19291(to D.J.A.)

References

1. Glagov S, et al. Compensatory Enlargement of Human Atherosclerotic Coronary Arteries. *N. Engl. J. Med.* 1987;316(22):1371-5.
2. Virmani R, et al. Atherosclerotic Plaque Progression and Vulnerability to Rupture: Angiogenesis as a Source of Intraplaque Hemorrhage. *Arterioscler. Thromb. Vasc. Biol.* 2005;25(10):2054-61.
3. Kolodgie FD. Pathologic assessment of the vulnerable human coronary plaque. *Heart.* 2004;90(12):1385-91.
4. Kolodgie FD, et al. The thin-cap fibroatheroma: a type of vulnerable plaque: The major precursor lesion to acute coronary syndromes. *Curr. Opin. Cardiol.* 2001;16(5):285-92.
5. Owens GK, et al. Molecular Regulation of Vascular Smooth Muscle Cell Differentiation in Development and Disease. *Physiol. Rev.* 2004;84(3):767-801.

6. Pullamsetti SS, et al. Novel and Emerging Therapies for Pulmonary Hypertension. *Am. J. Respir. Crit. Care Med.* 2014;189(4):394-400.
7. Rabinovitch M. Molecular pathogenesis of pulmonary arterial hypertension. *J. Clin. Invest.* 2012;122(12):4306-13.
8. Crosswhite P, and Sun Z. Molecular Mechanisms of Pulmonary Arterial Remodeling. *Mol. Med.* 2014;20(1):191-201.
9. Gomez D, and Owens GK. Smooth muscle cell phenotypic switching in atherosclerosis. *Cardiovasc. Res.* 2012;95(2):156-64.
10. Nishimura G, et al. δEF1 Mediates TGF-β Signaling in Vascular Smooth Muscle Cell Differentiation. *Dev. Cell.* 2006;11(1):93-104.
11. Yoshida T, et al. Myocardin Is a Key Regulator of CArG-Dependent Transcription of Multiple Smooth Muscle Marker Genes. *Circ. Res.* 2003;92(8):856-64.
12. Shankman LS, et al. KLF4-dependent phenotypic modulation of smooth muscle cells has a key role in atherosclerotic plaque pathogenesis. *Nat. Med.* 2015;21(6):628-37.
13. Chen P-Y, et al. Fibroblast growth factor (FGF) signaling regulates transforming growth factor beta (TGFβ)-dependent smooth muscle cell phenotype modulation. *Sci. Rep.* 2016;6(1):33407.
14. Harvey RP, et al. Homeodomain Factor Nkx2-5 in Heart Development and Disease. *Cold Spring Harb. Symp. Quant. Biol.* 2002;67(0):107-14.
15. Benson DW, et al. Mutations in the cardiac transcription factor NKX2.5 affect diverse cardiac developmental pathways. *J. Clin. Invest.* 1999;104(11):1567-73.
16. Tanaka M, et al. The cardiac homeobox gene Csx/Nkx2.5 lies genetically upstream of multiple genes essential for heart development. *Development.* 1999;126(6):1269-80.

17. Paffett-Lugassy N, et al. Heart field origin of great vessel precursors relies on nkx2.5-mediated vasculogenesis. *Nat. Cell Biol.* 2013;15(11):1362-9.
18. Ponticos M, et al. Regulation of Collagen Type I in Vascular Smooth Muscle Cells by Competition between Nkx2.5 and δEF1/ZEB1. *Mol. Cell. Biol.* 2004;24(14):6151-61.
19. Dritsoula A, et al. Molecular Basis for Dysregulated Activation of NKX2-5 in the Vascular Remodeling of Systemic Sclerosis: NKX2-5 MECHANISMS IN SCLERODERMA AND VASCULAR DISEASE. *Arthritis & Rheumatology.* 2018;70(6):920-31.
20. Ponticos M, et al. Col1a2 enhancer regulates collagen activity during development and in adult tissue repair. *Matrix Biol.* 2004;22(8):619-28.
21. Bou-Gharios G, et al. A potent far-upstream enhancer in the mouse pro alpha 2(I) collagen gene regulates expression of reporter genes in transgenic mice. *J. Cell Biol.* 1996;134(5):1333-44.
22. Antoniv TT, et al. Characterization of an Evolutionarily Conserved Far-upstream Enhancer in the Human α2(I) Collagen (COL1A2) Gene. *J. Biol. Chem.* 2001;276(24):21754-64.
23. Eastwood M, et al. A culture force monitor for measurement of contraction forces generated in human dermal fibroblast cultures: evidence for cell-matrix mechanical signalling. *Biochim Biophys Acta*. Nov 11 1994;1201:186-192.
24. Pashmforoush M, et al. Nkx2-5 pathways and congenital heart disease; loss of ventricular myocyte lineage specification leads to progressive cardiomyopathy and complete heart block. *Cell.* 2004;117(3):373-86.
25. Feil R, et al. Regulation of Cre Recombinase Activity by Mutated Estrogen Receptor Ligand-Binding Domains. *Biochem. Biophys. Res. Commun.* 1997;237(3):752-7.

26. Korshunov VA, and Berk BC. Smooth muscle apoptosis and vascular remodeling. *Curr. Opin. Hematol.* 2008;15(3):250-4.

27. Berk BC, and Korshunov VA. Genetic determinants of vascular remodelling. *Can. J. Cardiol.* 2006;22:6B-11B.

28. Rol N, et al. TGF-β and BMPR2 Signaling in PAH: Two Black Sheep in One Family. *Int. J. Mol. Sci.* 2018;19(9):2585.

29. Guignabert C, and Humbert M. Targeting transforming growth factor-β receptors in pulmonary hypertension. *Eur. Respir. J.* 2021;57(2):2002341.

30. Lane KB, et al. Heterozygous germline mutations in BMPR2, encoding a TGF-β receptor, cause familial primary pulmonary hypertension. *Nat. Genet.* 2000;26(1):81-4.

31. Chen PY et al. Smooth Muscle Cell Reprogramming in Aortic Aneurysms. *Cell Stem Cell.* 2020;26(4):542-557.e11.

32. Liu P, et al. Targeting the phosphoinositide 3-kinase pathway in cancer. *Nat. Rev. Drug Discov.* 2009;8(8):627-44.

33. Regan CP, et al. Erk5 null mice display multiple extraembryonic vascular and embryonic cardiovascular defects. *Proc. Natl. Acad. Sci. U. S. A.* 2002;99(14):9248-53.

34. Cuttano R, et al. KLF4 is a key determinant in the development and progression of cerebral cavernous malformations. *EMBO Mol. Med.* 2016;8(1):6-24.

35. Denton CP, et al. Fibroblast-specific expression of a kinase-deficient type II transforming growth factor β (TGFβ) receptor leads to paradoxical activation of TGFβ signalling pathways with fibrosis in transgenic mice. *J. Biol. Chem.* 2003;278:25109–19.

36. Denton CP, et al. Activation of Key Profibrotic Mechanisms in Transgenic Fibroblasts Expressing Kinase-deficient Type II Transforming Growth Factor-β Receptor (TβRIIΔk). *J. Biol. Chem.* 2005;280:16053–65.

37. Derrett-Smith EC, et al. Endothelial Injury in a Transforming Growth Factor β–Dependent Mouse Model of Scleroderma Induces Pulmonary Arterial Hypertension. *Arthritis Rheum.* 2013;65(11):2928-2939.
38. Samokhin AO, et al. NEDD9 targets COL3A1 to promote endothelial fibrosis and pulmonary arterial hypertension. *Sci. Transl. Med.* 2018;10(445):eaap7294.
39. Harmon AW, and Nakano A. Nkx2-5 lineage tracing visualizes the distribution of second heart field-derived aortic smooth muscle: Distribution of Shf-derived Smooth Muscle. *Genesis.* 2013;51(12):862-9.
40. Li X, et al. Control of germline stem cell differentiation by polycomb and trithorax group genes in the niche microenvironment. *Development.* 2016:dev.137638.
41. MacDonald BT, et al. Wnt/β-Catenin Signaling: Components, Mechanisms, and Diseases. *Dev. Cell.* 2009;17(1):9-26.
42. te Welscher P, et al. Progression of Vertebrate Limb Development Through SHH-Mediated Counteraction of GLI3. *Science.* 2002;298(5594):827-30.
43. Clark CD, and Lee K-H. Second heart field-specific expression of Nkx2-5 requires promoter proximal interaction with Srf. *Mech. Dev.* 2020;162:103615.
44. Sepulveda JL, et al. Combinatorial Expression of GATA4, Nkx2-5, and Serum Response Factor Directs Early Cardiac Gene Activity. *J. Biol. Chem.* 2002;277(28):25775-82.
45. Clark CD, et al. Evolutionary conservation of Nkx2.5 autoregulation in the second heart field. *Dev. Biol.* 2013;374(1):198-209.
46. Du M, et al. Nkx2-5 Is Expressed in Atherosclerotic Plaques and Attenuates Development of Atherosclerosis in Apolipoprotein E–Deficient Mice. *J. Am. Heart. Assoc.* 2016;5(12):e004440.

47. Zimmermann M, et al. Analysis of region specific gene expression patterns in the heart and systemic responses after experimental myocardial ischemia. *Oncotarget.* 2017;8(37):60809-25.
48. Deng H, et al. MEKK3-TGFβ crosstalk regulates inward arterial remodeling. *Proc Natl Acad Sci U S A.* 2021;118(51):e2112625118.
49. Zheng B, et al. Ligand-Dependent Genetic Recombination in Fibroblasts. *Am. J. Pathol.* 2002;160(5):1609-17.
50. Gareus R, et al. Endothelial Cell-Specific NF-κB Inhibition Protects Mice from Atherosclerosis. *Cell Metab.* 2008;8(5):372-83.
51. Kiermayer C, et al. Optimization of spatiotemporal gene inactivation in mouse heart by oral application of tamoxifen citrate. *Genesis.* 2007;45(1):11-6.
52. Chamley-Campbell JH, et al. Phenotype-dependent response of cultured aortic smooth muscle to serum mitogens. *J. Cell Biol.* 1981;89(2):379-83.
53. Vandesompele J, et al. Accurate normalization of real-time quantitative RT-PCR data by geometric averaging of multiple internal control genes. *Genome Biol.* 2002;3(7):research0034.1.

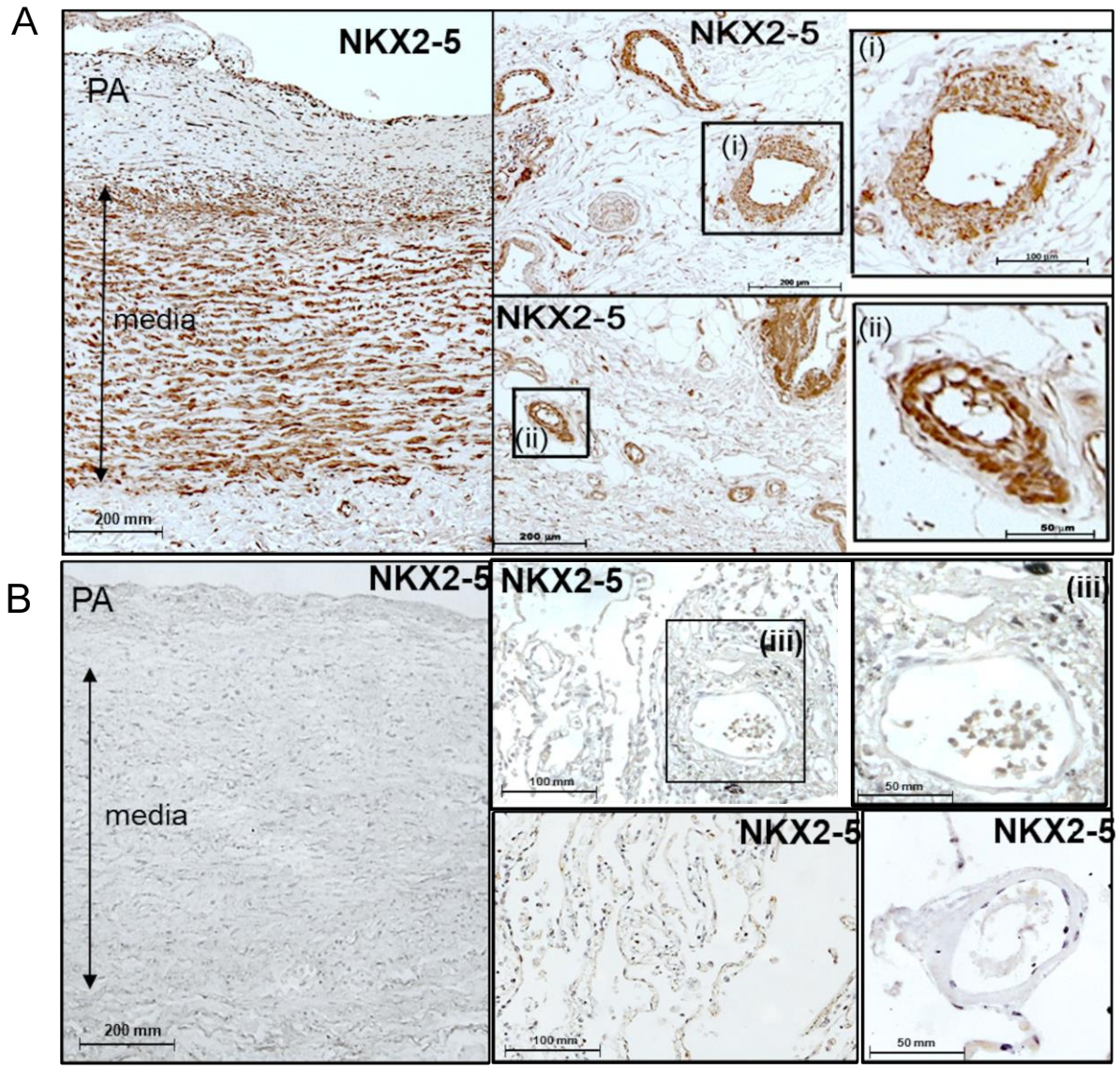

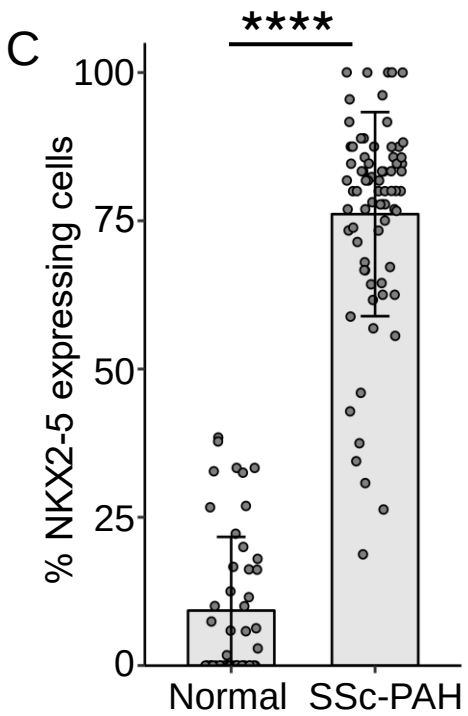

Figure 1. NKX2-5 is expressed by VSMC in scleroderma patients with PAH. Lung tissue sections were immunostained for NKX2-5 (brown) and counterstained with hematoxylin. Examples of large pulmonary arteries (PA) (>100mm, left panel and inset i) and medium (40-70mm inset ii) are highlighted, but small arteries (20-40mm) can also be seen. **(A)** SSc-PAH patients **(B)** Healthy lung tissue **(C)** NKX2-5 expression was quantified by counting positive cells in sections of PAH or control pulmonary tissue and expressed as a percentage of total cells. For each condition 75 vessels 20-100 µm were counted in total from 5 different subjects. **** P<0.0001 by paired two-tailed Student's *t* test. Error bars, ± s.d.

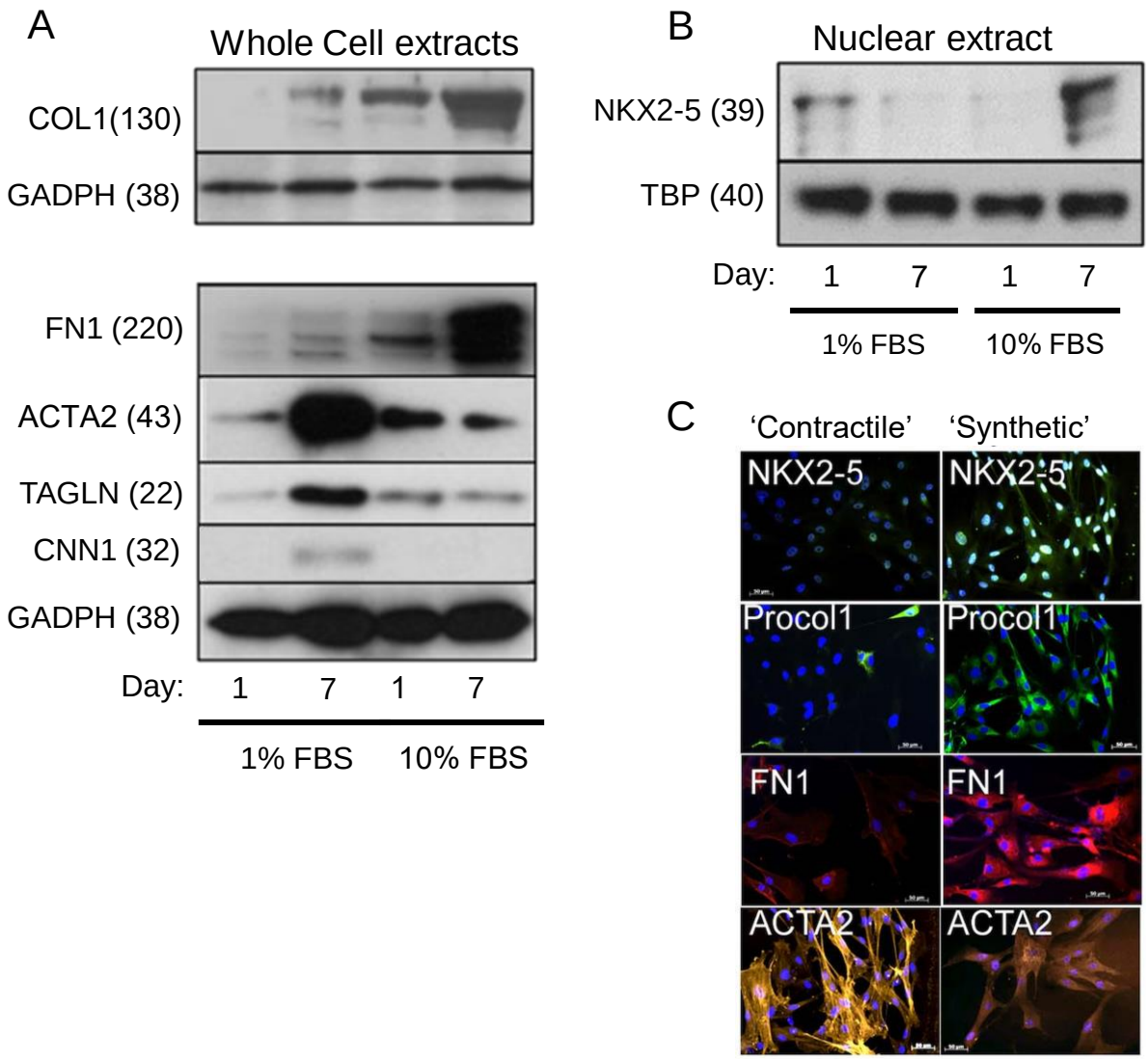

Figure 2. NKX2-5 expression is associated with the synthetic phenotype in HPASMC. HPASMC were cultured *in vitro* under conditions favouring the contractile or synthetic phenotype, over 7 days. (**A**) Protein expression levels of NKX2-5, synthetic cell markers COL1, and FN1, and contractile cell markers ACTA2, CNN1 and TAGLN were determined by Western blotting. A representative blot from three independent experiments is shown. Statistical significance was examined with a two-way ANOVA (supplementary figures). The effect of FBS and the effect of time are both significant at $P < 0.05$ for all genes. All genes come from the same samples run on different, but concurrent blots, except for COL1, which was run on a separate occasion. (**B**) Nuclear extracts were used to quantify NKX2-5 expression via Western blotting with the E1Y8H antibody. A representative blot from two independent experiments is shown. Substantial expression of NKX2-5 is only observed after prolonged culture in serum ($P<0.05$ via t-test). NKX2-5 and TBP were run on different, but concurrent blots (**C**) Immunofluorescence was carried out on contractile (7 days in 1% FBS) or synthetic (7 days in 10% FBS) HPASMC using specific antibodies for NKX2-5 (Alexa488, green), intracellular Pro-collagen type I (Procol1, Alexa488 green), FN1 (Alexa594, red), ACTA2 (Cy3, orange) and DAPI (blue). Nuclear expression of NKX2-5 was concomitant with high COLI1 and FN1 expression in synthetic but not contractile HPASMC. High levels of organized ACTA2 expression were only visible in contractile cells. All protein molecular weights are given as KDa in (parentheses).

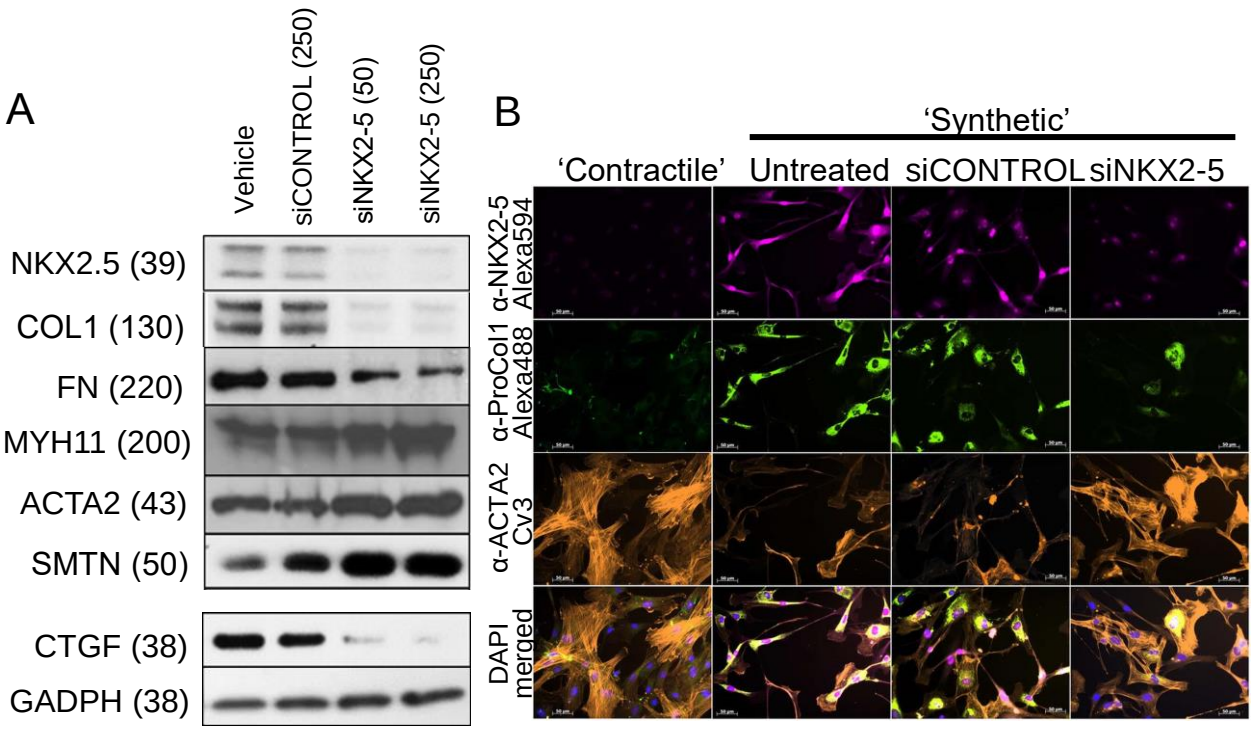

Figure 3. NKX2-5 expression is needed to maintain the contractile phenotype. HPASMC cultured in serum for 7 days were treated with siRNA against NKX2-5 (50nM or 250nM) or scrambled siCONTROL (250nM) for 72h. The densitometry results were analysed with ANOVA (supplementary figures). The effect of siNKX2-5 is significant at $P<0.05$ for all genes. (**A**) Representative western blot (n=3) for contractile and synthetic markers, (NKX2-5 antibody: E1Y8H). NKX2-5 downregulation supresses COL , CTGF and FN1, but increases MYH11, ACTA2 and SMTN. For all proteins, the same samples were run on different, but concurrent western blots. (**B**) The expression of NKX2-5, pro-COL1 and ACTA2, after NKX2-5 knockdown was investigated by immunofluorescence. NKX2-5 knockdown results in reduced pro-COL1 expression, while ACTA2 expression and organization into myofilaments is partially restored. All protein molecular weights are given as KDa in (parentheses).

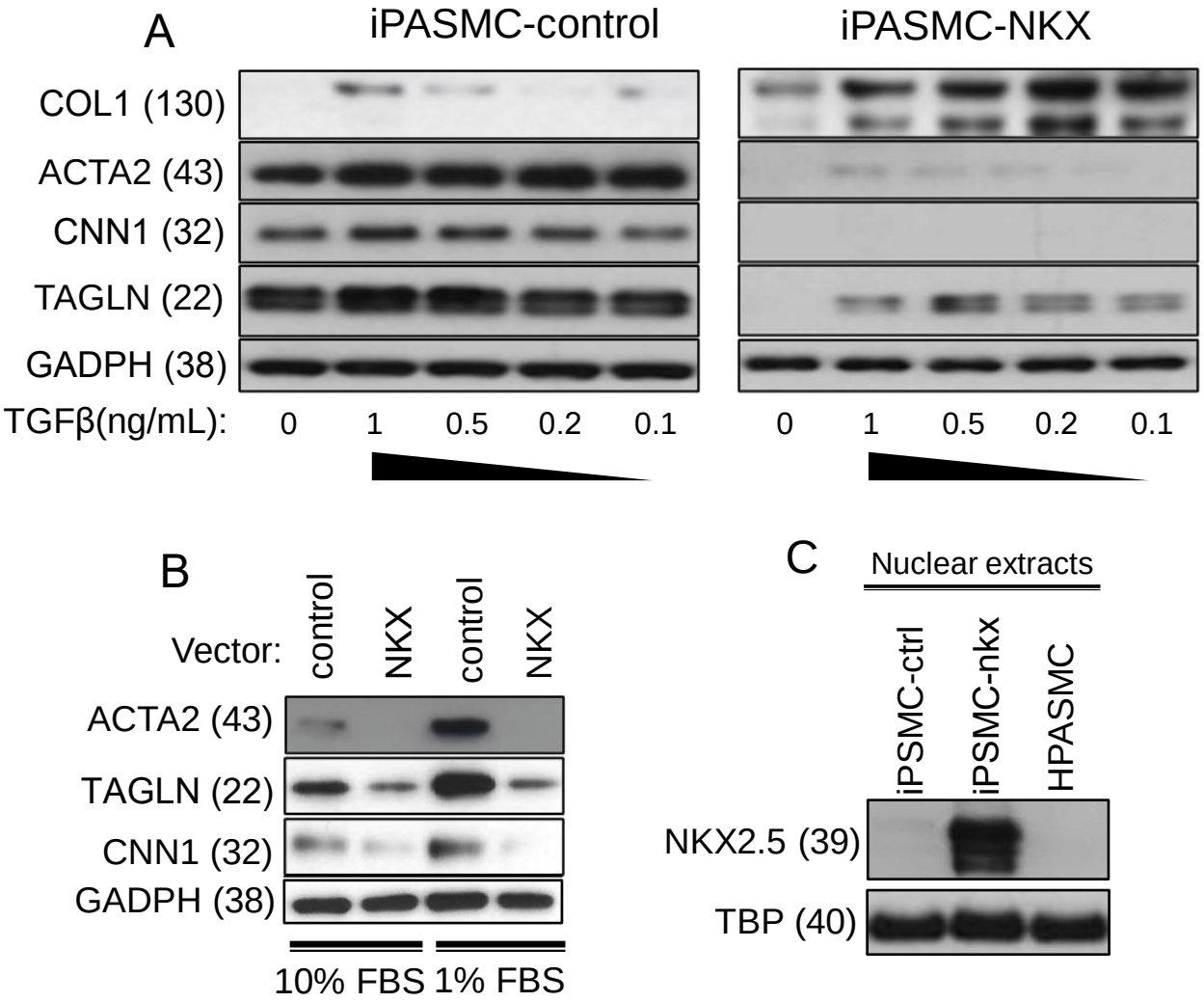

Figure 4. NKX2-5 expression locks SMC into the synthetic phenotype. (A) An immortalized HPASMC (iPASMC) cell line was transduced with an NKX2-5 Lentiviral vector (iPASMC-NKX) or a control vector (iPASMC-control). The transduced cells were cultured for 7 days in growth media with 1% FBS and various concentrations of TGFβ to induce contractile marker expression. A two-way ANOVA analysis of these results (supplementary figures) confirmed that the differences between Control and transduced cells were highly significant ($P<0.01$). Control and NKX samples were always run on the same blot. For all proteins, the same samples were run on different, but concurrent western blots. **(B)** Primary HPASMC, were transduced with either an NKX2-5 lentiviral vector (NKX) or a control vector. After transduction and selection, the cells were cultured for 7 days in media with either at 10% FBS and low density to induce the synthetic phenotype or 1% FBS and high density to activate the contractile phenotype. T-test analysis (n=2) showed reduction in ACTA2 and TAGLN protein expression after NKX2-5 transduction is significant in both 1% and 10% FBS ($P<0.01$), but the CNN1 reduction is only significant in 1% FBS ($P<0.01$). **(C)** Western blot analysis of NKX2-5 expression in nuclear extracts from iPASMC-NKX and iPASMC-control (iPASMC-ctrl). Contractile HPASMC are also included as a reference. In (B) and (C) different genes used the same samples run on different but concurrent blots.

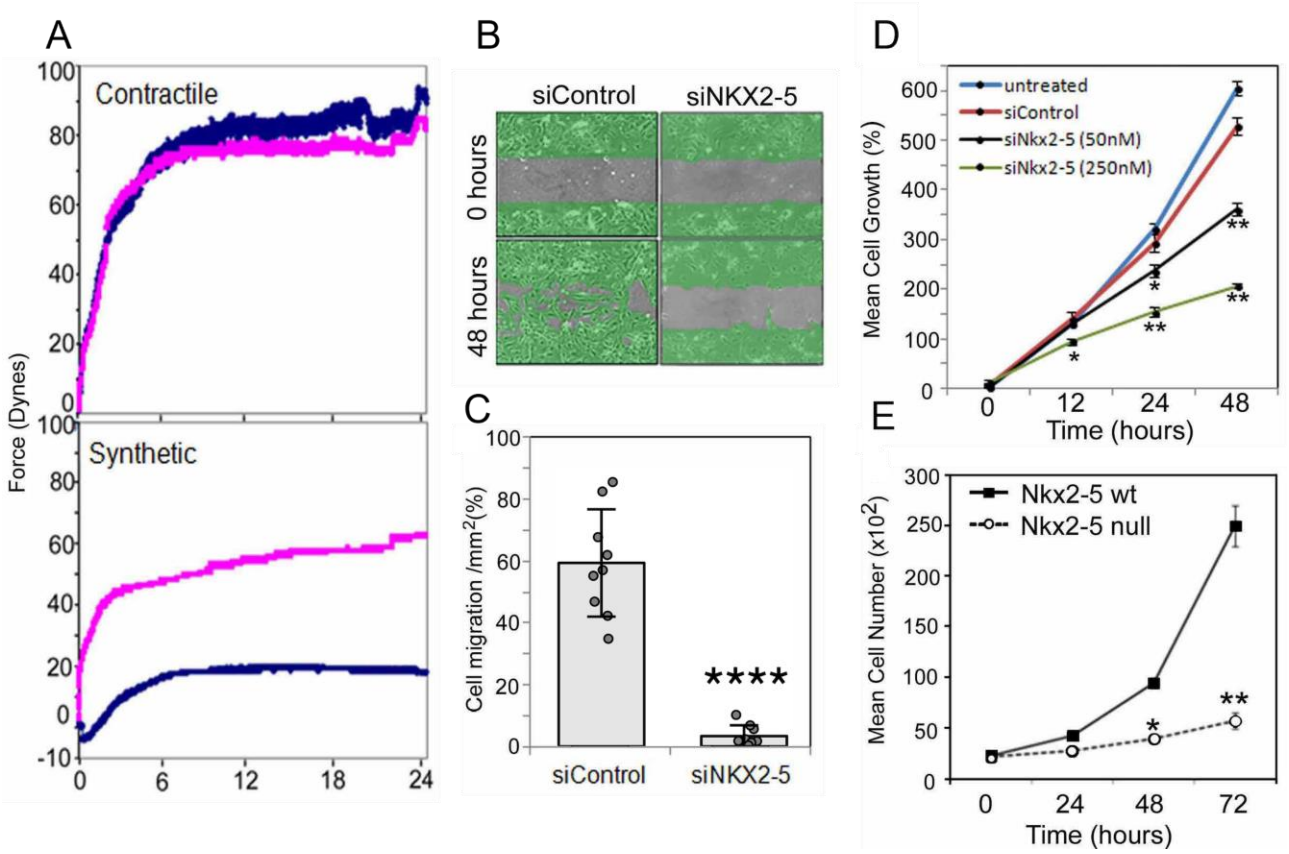

Figure 5. NKX2-5 inhibits VSMC contraction and promotes migration and proliferation. NKX2-5 knockdown was accomplished with siRNA in contractile (1% FBS) or synthetic (10% FBS) HASMC. Scrambled oligonucleotides were used as control (siCONTROL). (**A**) Force of contraction exerted on a 3-dimentional collagen gel seeded with treated HASMC was measured continuously using a tensioning culture force monitor over 24hours. siNKX2-5 treated synthetic HASMC (red) augmented contractility compared to siCONTROL treated synthetic HASMC (blue). (**B**) NKX2-5 knockdown in synthetic HASMC inhibited cell migration into a scratch wound over 48 hours compared to control. (**C**) Nine separate scratch wound experiments were quantified for cell migration into the scratch. **** P<0.0001 by paired two-tailed Student's *t* test. Error bars, ± s.d. (**D**) Cell proliferation of synthetic HASMC over 48 hours was measured after no treatment (blue) siCONTROL treated (red) siNKX2-5 (50nM, black) or siNKX2-5 (250nM green). Statistical significance was confirmed at P<0.05 with ANOVA. * P<0.05, ** P<0.01 by post-hoc paired two-tailed Student's *t* tests. Error bars, ± s.e.m. (**E**) NKX2-5 was deleted in mouse synthetic aortic SMC (explanted from NKX2-5^{flox}Col1a2^{CreERT} mice, n=3 – see methods) by infection with either Ad.CRE or Ad.GFP (control) (MOI 100). Cell proliferation was measured in triplicate for each cell line over 72 hours. Statistical significance at P<0.05 was confirmed by ANOVA. * P<0.05 ** P< 0.01 by post-hoc unpaired two-tailed Student's *t* tests. Error bars, ± s.e.m.

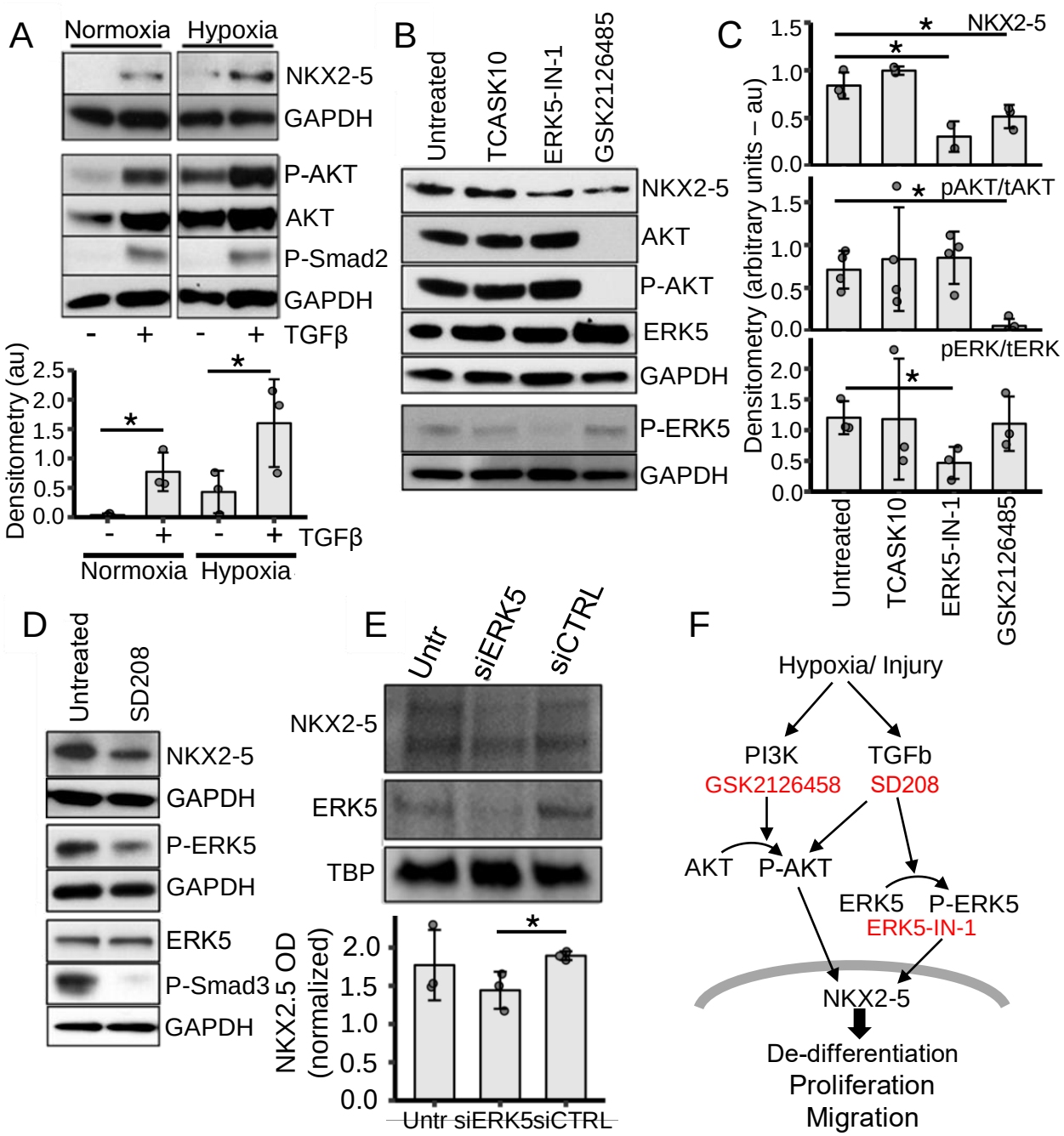

Figure 6. Signalling pathways that result in NKX2-5 activation. (**A**) HPASMC cultured for 2days, in synthetic conditions (10% FBS, low density), in Hypoxia (1% oxygen) or normoxia, with or without TGFb1 (4ng/ml). Total NKX2-5 protein was analyzed by densitometry (n=3, au = arbitrary units) (**B**) Synthetic HPASMC expressing NKX2-5 were treated with inhibitors for ASK1 (TS ASK10), ERK5 (ERK5-IN-1) and PI3K (GSK2126458). (**C**) Densitometry quantification (n=3) for of (B). (**D**) HPASMC grown under synthetic conditions, treated with a TGFβ Receptor II inhibitor (SD208). **(E)** Western blots were performed using nuclear extracts from HPASMC grown under synthetic conditions and treated with vehicle, siRNA (50 nM final concentration) against ERK5 (siERK5) or control siRNA (siCTRL) and quantified by densitometry (n=3) Error bars, ± s.d. For all blots with multiple proteins the same samples were run on different, but concurrent western blots. **(F)** Potential signalling mechanism for the activation of NKX2-5 in HASMC: Combinations of hypoxia and injury aided by TGFβ reactivate NKX2-5, via the PI3K and ERK5 pathways. Statistical significance was assessed by paired two-tailed Student's *t* test (* P<0.05).

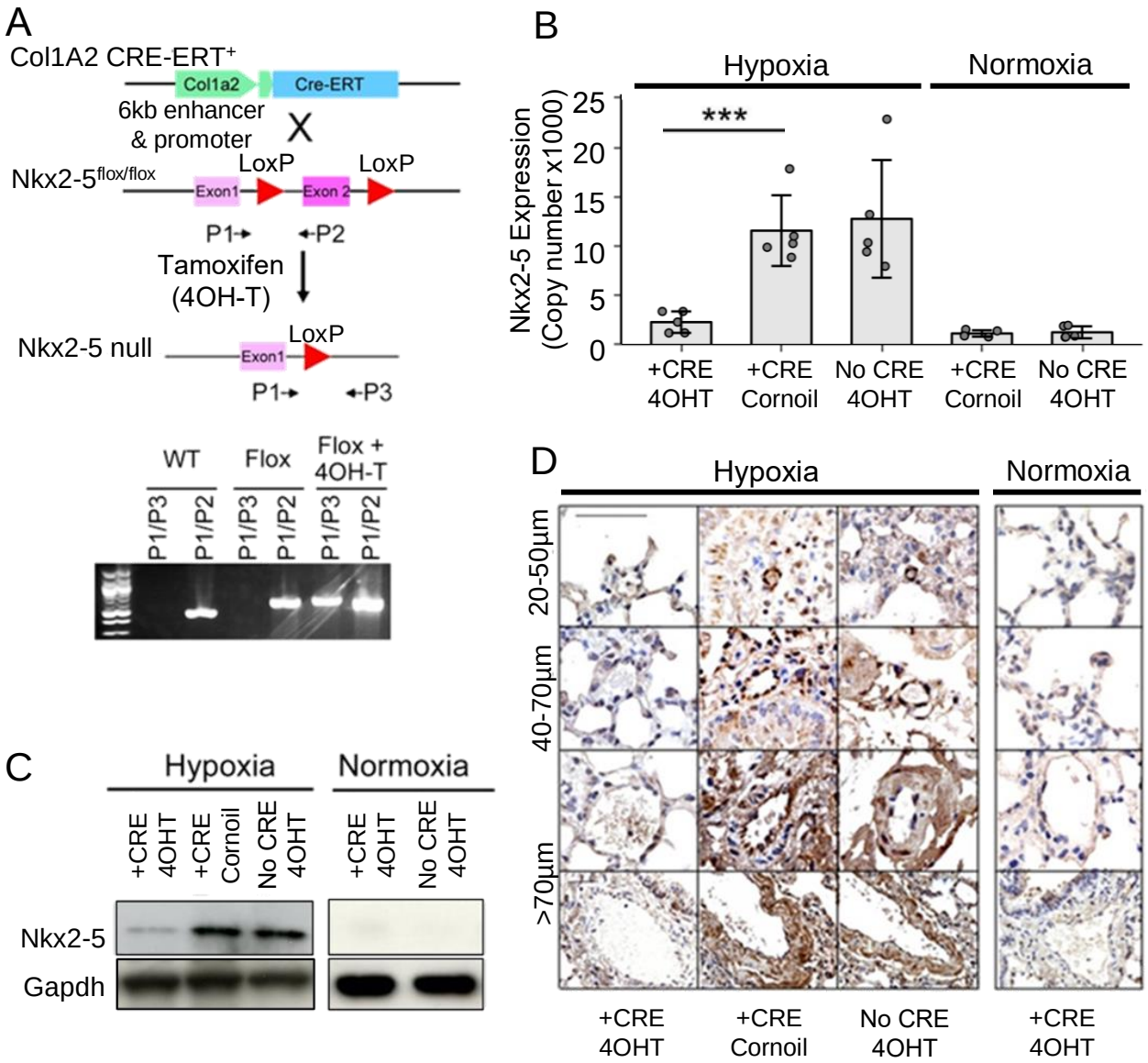

Figure 7. Targeted Nkx2-5 deletion in the chronic hypoxia model of Pulmonary Hypertension. (**A**) Strategy for conditional deletion of NKX2-5 in collagen-producing cells using the collagen type Ia2 enhancer to drive expression of Cre recombinase upon administration of Tamoxifen (4OH-T) in adult male mice in the chronic hypoxia model of PH (Col1a2Cre-ER). PCR primers (P1,P2 and P3) were designed to detect Nkx2-5 deletion as described in the methods. (**B**) Nkx2-5 mRNA levels in pulmonary arteries of mice (n=8 per group) under hypoxia or normoxia for 21 days. *** P<0.001 by unpaired two-tailed Student's *t* test. Error bars, ± s.d. (**C**) Nkx2-5 protein levels were analysed by SDS-PAGE in total lung lysates from mice in hypoxia or normoxia. The samples from the hypoxia experiment to determine Nkx2-5 and GAPDH were run on different, but concurrent western blots. (**D**) Expression of Nkx2-5 (brown DAB staining) in lung vessels in null mouse and control groups were determined via immunohistochemistry under normoxia and hypoxia. Representative images of small (20-50mM), medium (40-70mM) and large arteries (>70mM) are shown. Scale Bar, 100mM.

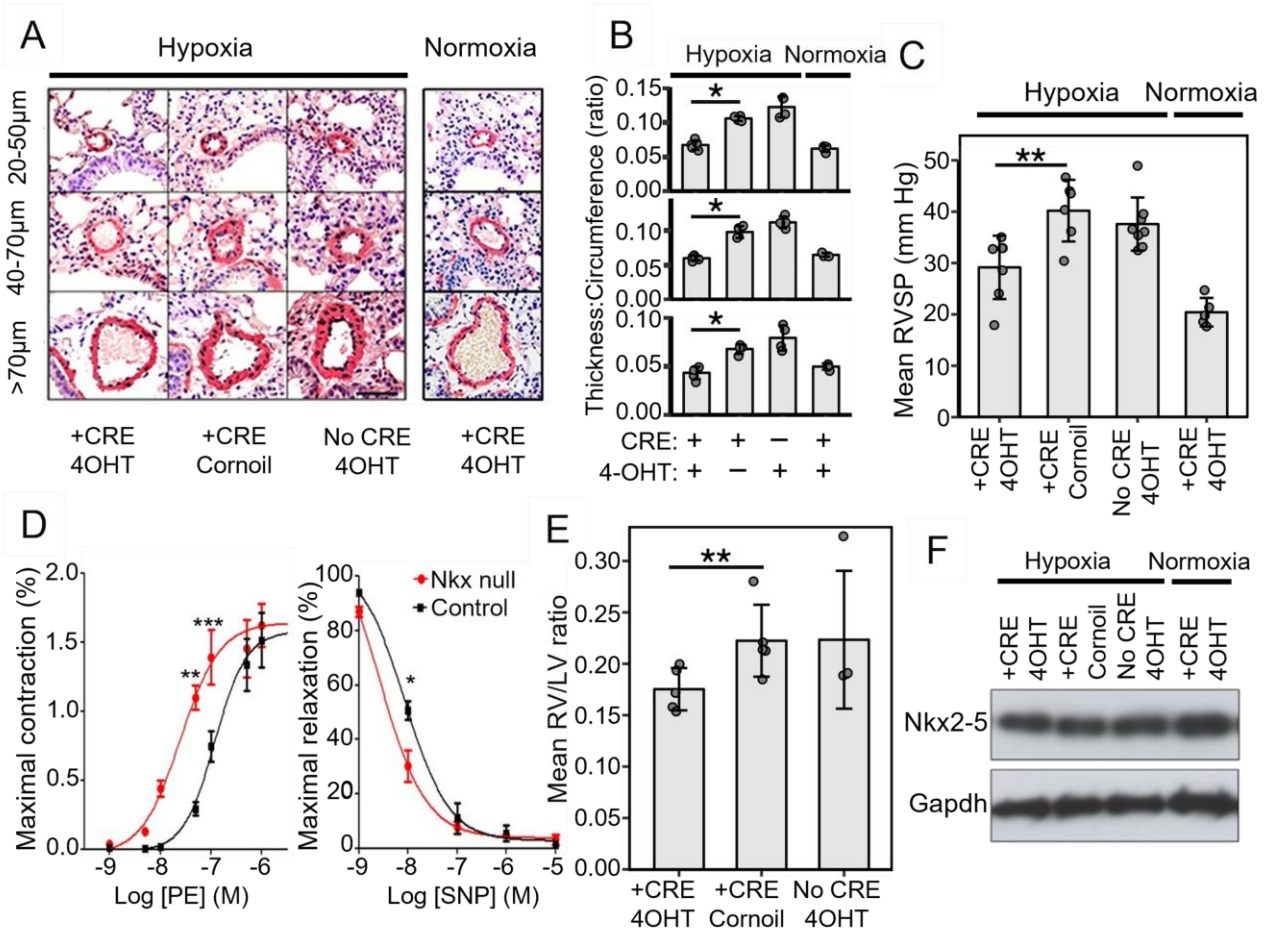

Figure 8. Nkx2-5 deletion ameliorates symptoms of chronic hypoxia-induced pulmonary vascular remodelling. Nkx2-5 null (Nkx2-5^{flox} Cre^{+} 4OH-T) or control male mice were exposed in hypoxia or kept under normoxia for 21 days (see fig 7 and methods). (**A**) Sections of the entire left lobe of the mouse lungs were immunostained for ACTA2 to visualise vessels. Representative images of small (20-50mm), medium (40-70mm) and large arteries (>70mm) are shown (Scale Bar, 100µm) (**B**) Muscularisation (thickness: circumference ratio) of the arterial wall of pulmonary vessels was analysed (n=5 mice per group and 300-500 vessels per group) and quantified under hypoxia and normoxia . * P<0.05 by unpaired two-tailed Student's *t* test, Error bars and s.d shown. (**C**) RSVP measurements in Nkx2-5 null and control mouse groups under hypoxia and normoxia (n=8 mice per group). ** P<0.01 by unpaired two-tailed Student's *t* test, Error bars, and s.d shown. (**D**) Cumulative concentration response curves to (phenylephrine) PE or sodium nitroprusside (SNP) in endothelium-intact first and second order pulmonary artery segments from Nkx2-5-null (red n=4) or Control (black n=5) mice. Contraction in response to PE concentration is expressed as mean ± SEM percentage. Relaxation is expressed as mean ± SEM percentage reversal of PE-induced tone. Statistical significance at P<0.05 was confirmed by ANOVA. *P < 0.05, **P < 0.01, ***P < 0.001, by post-hoc unpaired two-tailed Student's t-tests. (**E**) Mean RV/LV ratio as a standard measure of right ventricular hypertrophy. ***P < 0.001 by unpaired two-tailed Student's t-test. (**F**) Expression of Nkx2-5 in whole heart tissue. Representative blot from 3 different experiments. No statistically significant differences observed. Nkx2-5 and Gapdh were run on different but concurrent blots.